Scheduler Algorithms for MU-MIMO

WISSAM MOUSTAFA AND RICHARD MUGISHA
MASTER´S THESIS
DEPARTMENT OF ELECTRICAL AND INFORMATION TECHNOLOGY
FACULTY OF ENGINEERING | LTH | LUND UNIVERSITY

Scheduler Algorithms for MU-MIMO

By

Wissam Moustafa and Richard Mugisha

Department of Electrical and Information Technology
Faculty of Engineering, LTH, Lund University
SE-221 00 Lund, Sweden

LUND UNIVERSITY

ERICSSON

2017

Abstract

In multi-user multiple input multiple output (MU-MIMO), the complexity of the base-station scheduler has increased further compared to single-user multiple input multiple output (SU-MIMO). The scheduler must understand if several users can be spatially multiplexed in the same time-frequency resource. One way to spatially separate users is through beamforming with sufficiently many antennas.

In this thesis work, two downlink beamforming algorithms for MU-MIMO are studied: The first algorithm implements precoding without considering inter-cell interference (ICI). The second one considers it and attempts to mitigate or null transmissions in the direction of user equipments (UEs) in other cells. The two algorithms are evaluated in SU-MIMO and MU-MIMO setups operating in time division duplex (TDD) mode and serving with single and dual-antenna terminals. Full-Buffer (FB) and file transfer protocol (FTP) data traffic profiles are studied. Additionally, various UE mobility patterns, UE transmit antenna topologies, sounding reference signal (SRS) periodicity configurations, and uniform linear array (ULA) topologies are considered. Simulations have been performed using a system level simulation framework developed by Ericsson AB.

Another important part of this thesis work is the functional verification of this simulation framework, which at the time of writing is still undergoing development.

Our simulation results show that in SU-MIMO, the second algorithm, which considers ICI, outperforms the first one for FB traffic profile and all UE speeds, but not for FTP traffic profile and medium (30 km/h) or high (60 km/h) UE speeds. In this case, the first algorithm, which does not consider ICI, can be used with advantage. In MU-MIMO, cell downlink throughput gains are observed for the second algorithm over the first one for low and medium system loads (number of users). For both algorithms, the cell throughput is observed to decrease with increasing UE speed and sounding periodicity.

Acknowledgments

It is great honor and pleasure for us to express our deepest gratitude to our supervisor Fredrik Tufvesson and examiner Fredrik Rusek, of the Department of Electrical and Information Technology, Lund University, for their valuable supervision and guidance throughout the whole study. Special acknowledgement is extended to our co-supervisors Jose Flordelis of the Department of Electrical and Information Technology, Lund University, and José María García Perera of Ericsson AB, for their valuable assistance, motivation, and guidance throughout the thesis. Our sincere gratitude to Ericsson AB, Lund Branch for their facilitation in providing office space, data and a great team of professionals who assisted us at every chance they got. Also, we are profoundly grateful to the Swedish Institute for awarding us full-time scholarships to pursue our master degrees. Last but not least, we would like to thank our families and friends in Syria, Rwanda and Sweden for all the love and support.

Wissam Moustafa, Lund, June 2017
Richard Mugisha, Lund, June 2017

Contents

Preface

In this thesis work, all parts have been done by both authors together.

List of figures

List of tables

List of acronyms

- **2D** Two-Dimensional
- **3D** Three-Dimensional
- **3GPP** Third-Generation Partnership Project
- **BLER** Block Error Rate
- **BS** Base Station
- **CP** Cyclic Prefix
- **CRC** Cyclic Redundancy Check
- **CRS** Cell-specific Reference Signals
- **CSI** Channel State Information
- **CSI-RS** CSI Reference Signals
- **DCI** Downlink Control Information
- **DL** Downlink
- **DM-RS$_{(DL)}$** Downlink Demodulation Reference Signals
- **DM-RS$_{(UL)}$** Uplink Demodulation Reference Signals
- **FDD** Frequency Division Duplex
- **FTP** File Transfer Protocol
- **GSM** Global System for Mobile communication
- **HARQ** Hybrid ARQ
- **HSPA** High Speed Packet Access
- **ICI** Inter-Cell Interference
- **ITU** International Telecommunication Union
- **LAA** Licensed Assisted Access
- **LTE** Long Term Evolution
- **MCS** Modulation Coding Scheme
- **MIMO** Multiple Input Multiple Output
- **MMSE** Minimum Mean Square Error
- **MU-MIMO** Multi-User MIMO

- **OFDM** Orthogonal Frequency Division Multiplexing
- **PBCH** Physical Broadcast Channel
- **PDCCH** Physical Downlink Control Channel
- **PDCSH** Physical Downlink Shared Channel
- **PF** Proportional Fair
- **PRB** Physical Resource Block
- **PUCCH** Physical Uplink Control Channel
- **PUSCH** Physical Uplink Shared Channel
- **QAM** Quadrature Amplitude Modulation
- **QoS** Quality of Service
- **QPSK** Quadrature Phase Shift Keying
- **RBG** Resource Block Group
- **RR** Round Robin
- **SC-FDMA** Single Carrier Frequency Division Multiple Access
- **SCM** Spatial Channel Model
- **SINR** Signal to Interference Noise Ratio
- **SRS** Sounding Reference Signal
- **SU-MIMO** Single-User MIMO
- **TDD** Time Division Duplex
- **TTI** Transmission Time Interval
- **UE** User Equipment
- **UL** Uplink
- **ULA** Uniform Linear Array
- **WCDMA** Wide Band Code Division Multiple Access
- **ZF** Zero Forcing

Popular Science Summary

Scheduling in modern wireless standards, e.g., 3G, 4G and future 5G, can be defined as the task of allocating time and frequency resources by the base station (BS) to each user equipment (UE) that wants to engage in communication. Resources are allocated every transmission time interval (TTI), which is typically one millisecond. There exist both uplink (from the UEs to the BS) and downlink (from the BS to the UEs) resource schedulers implemented in the e-Node B, i.e., the base station (BS) in Long Term Evolution (LTE).

The aim of this thesis work is to study how various communication techniques proposed for 5G can increase the overall system throughput of the downlink (DL) when a realistic resource scheduler is used. In particular, we consider: (i) Beamforming, (ii) Multi-user multiple input multiple output (MU-MIMO), and (iii) Inter-cell interference (ICI) mitigation.

Beamforming can be achieved by deploying a large number of antenna elements at the BS with the aim of increasing the signal to interference noise ratio (SINR) towards the UE. Contrary to single-user multiple input multiple output (SU-MIMO), in MU-MIMO more than one UE are scheduled for transmissions in the same time-frequency resource; this is possible by judiciously pairing various UEs which are spatially sufficiently separated (according to some metric that we will define later). ICI mitigation can be achieved by means of proper precoding at BS where the precoder attempts to mitigate the interfering signal from BS towards UEs belonging to neighboring cells.

In this thesis work, we investigate the performance of two scheduler algorithms for MU-MIMO, using SU-MIMO as baseline. The first algorithm does not consider ICI while the second one does. Dual layer beamforming (that is, two independent data streams are transmitted to each UE) and time division duplex (TDD) are assumed. In TDD mode the BS acquires the channel information from sounding reference signals (SRS) transmitted in the uplink (UL) and, by virtue of channel reciprocity, reuses the so-obtained channel information in the downlink.

The performance evaluation of the two algorithms is based on the following parameters: UE Traffic profile, UE speed, SRS UL antenna configuration, SRS parameters, and BS antenna topology.

- UE speed includes 3,30, and 60 km/h.

- UE traffic profile includes full-buffer (FB) and file transfer protocol (FTP). With FB traffic profile, UEs send/receive data to/from the BS all the time, while this is not the case in the FTP traffic profile case. Some examples of FTP traffic profiles may include chatty, video, VoIP, web, etc.
- SRS UL antenna configuration includes: (i) Two SRS, in which each UE sends two SRS to the BS from two antennas, (ii) one SRS with antenna selection, in which each UE alternately sends one SRS to the BS from each of two antennas, and (iii) one SRS without antenna selection, in which each UE sends one SRS to the BS from only one antenna. For two SRS UE case (note that in the downlink two layers, and hence two UE antennas, are always used).
- SRS parameters include SRS bandwidth and SRS periodicity. In this thesis work, full-bandwidth SRS (20 MHz) with various SRS periodicities such as 5 ms, 10 ms, 20 ms are considered.
- BS antenna topology includes 8 and 64 antenna elements at the BS.

The main result of this thesis work is that in both SU-MIMO and MU-MIMO with FB traffic profile, it is better to use the second algorithm which considers ICI rather than the first one-which does not. However, with FTP traffic profile, this is not always the case.

1. Introduction

This chapter is organized into six sections: Background and motivation, project aims and main challenges, approach and methodology, previous related work, limitations, and thesis outline.

1.1. Background and motivation

Scheduling in modern wireless standards, e.g., 3G, 4G and future 5G, can be defined as the task of allocating time and frequency resources by the base station (BS) to each user equipment (UE) that wants to engage in communication.

In multi-user multiple input multiple output (MU-MIMO), the complexity of the base station (BS) scheduler has increased compared to single-user multiple input multiple output (SU-MIMO). It must understand if several users can be spatially multiplexed by using the same time-frequency resources for these different users. One way to determine if several users are spatially separated and co-scheduled using the same time-frequency resources is through a beamformed system with sufficient antennas.

The scheduler algorithm should be very efficient so that it can serve as much user equipments (UEs) as possible and provide good cell throughput by sharing all the available time-frequency resources with different UEs. Hence, there is a need to design a scheduler which is optimized so that:

- The available time-frequency resources are utilized and assigned to maximize the cell data throughput (no wastage of resources).
- More UEs are scheduled within the same transmission time interval (TTI), while maintaining the block error rate (BLER) target.
- UE specific quality of service (QoS) is possible, i.e. all the UEs in the cell are given a chance to be scheduled according to its grade of service.

1.2. Project aims and main challenges

The main objective of this thesis work is to analyze and evaluate the advantages and drawbacks of two MU-MIMO scheduler algorithms, in various BS and UE configurations, with the main objective of maximizing the cell throughput of the system. Later, performance comparisons of MU-MIMO against SU-MIMO are carried out by setting SU-MIMO as a baseline.

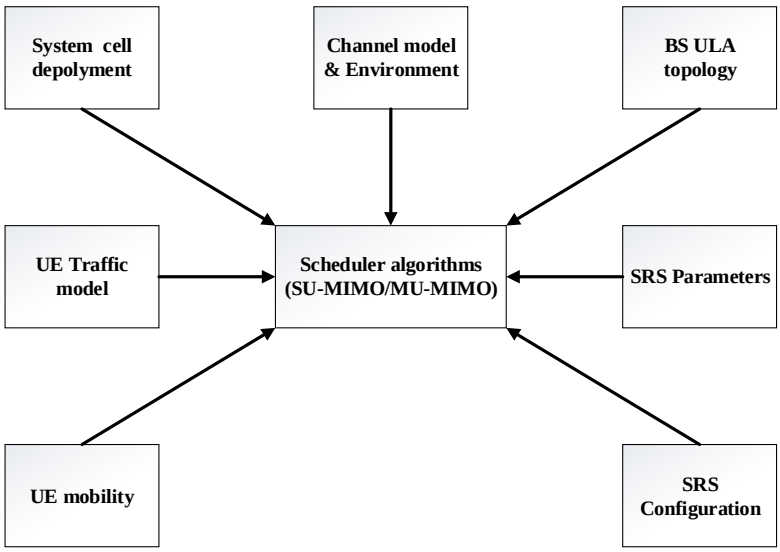

Figure 1.1: Scheduler algorithms challenges (SU-MIMO/MU-MIMO)

As shown in Fig.1.1, to assess the performance of the scheduler algorithms for both SU-MIMO and MU-MIMO, the following inputs are needed:

- Channel model: The channel model includes the two dimensional (2D) and three dimensional (3D) spatial channel models (SCM), which are used with 8 and 64 antenna elements at the BS, respectively.
- Environment: The simulation environment can be broadly classified as suburban-macro, urban-macro, and urban-micro. In this thesis work, we use only urban-macro.

- System cell deployment: The system deployment includes the cell layout, the number of sites, the number of sectors/cells per site and the number of users per sector/cell.
- UE traffic model: The UE traffic model includes full-buffer (FB) and file transfer protocol (FTP) traffic profiles. FTP traffic is a kind of bursty traffic.
- UE mobility: The UE mobility refers to the users' speed e.g., 3 km/h, 30 km/h, 60 km/h, etc.
- SRS UL antenna configuration: The SRS UL antenna configuration includes UE with two simultaneous SRS transmission (2 SRS UE), UE with one SRS transmission with antenna selection/switching (1 SRSAS UE) and UE with one SRS transmission without antenna selection/switching (1 SRSWOAS UE).
- SRS parameters: The SRS parameters include both full-bandwidth and sub-bands SRS configurations with different SRS periodicity e.g. 5 ms, 10 ms, 20 ms, etc.
- BSULA topology: The base station uniform linear array (BSULA) includes a BS with 8 and 64 antenna elements.

A main challenge of this thesis work was to verify the correct implementation of the system simulator functionalities (verification of the system simulator). Some important issues were found during our thesis work, and those were reported to Ericsson AB and investigations are ongoing.

1.3. Approach and methodology

This thesis work was carried out through the following steps as illustrated in Fig. 1.2:

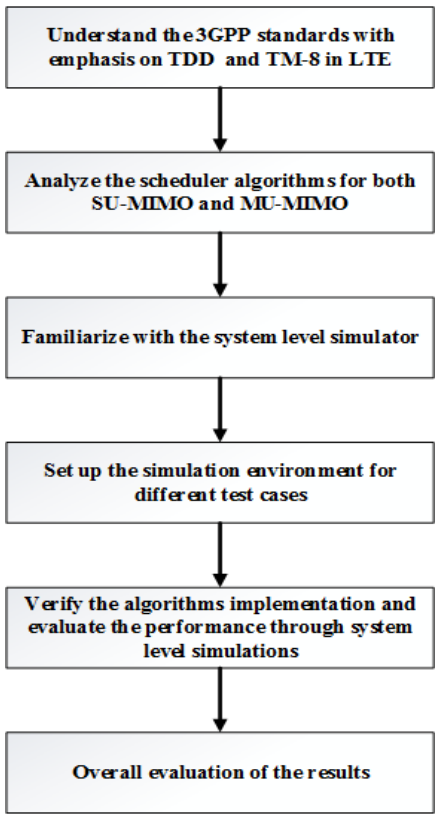

Figure 1.2: Flow diagram of the methodology

a. This thesis work is based on the 3GPP standards with emphasis on TDD and Transmission mode 8 (TM-8) in LTE.

b. A deep analysis of the used scheduler algorithms for both SU-MIMO and MU-MIMO is needed since the overall system performance is mainly based on them.

c. The system level simulator is used to simulate the behavior of real radio networks such as GSM, WCDMA, LTE, etc. In this case, there is no need to build a physical radio network in advance which is an advantage in terms of adjustments/flexibility, time, and costs.

d. Building and preparing the simulation environment for different test cases requires some input parameters from the e-Node B and UEs as well as the channel.

e. Verify and evaluate the performance by simulating the algorithms for different scenarios as mentioned in Section 1.2.

f. Analyze the simulation results as a function of the number of UEs that are scheduled, and provide some recommendations based on the performance.

1.4. Previous related work

LTE has been developed by the Third-Generation Partnership Project (3GPP) and was adopted to be the promising broadband technology for 4G and future 5G mobile standards to replace both GSM (2G) and WCDMA/HSPA (3G) standards. Initially, the International Telecommunication Union (ITU) specifies LTE data rates to be up to 100Mbps and 1Gbps in high and low mobility applications, respectively, for fourth generation (4G) mobile communication systems [1].

To meet those requirements, SU-MIMO and MU-MIMO schemes are used in LTE technology. The only difference between those two is that in the latter case, the e-Node B in LTE (the BS) sends independent data streams to multiple users simultaneously in the same time-frequency resources, while in the former case, each user is allocated by the BS its own time-frequency resources. MU-MIMO can be achieved by spatially separating multiple users.

Different multi-antenna technologies for LTE-Advanced are briefly discussed in [2], including design targets, deployment scenarios, multi-antenna setups, downlink and uplink design, and performance assessment based on cell spectral efficiency and cell-edge user spectral efficiency. It was shown in [2] that the cross-polarized antenna setup at the base station outperforms the co-polarized one in terms of cell spectral efficiency while the opposite is true for cell edge user spectral efficiency case. More techniques related to MU-MIMO in LTE-Advanced are also introduced in [3], [4], including design challenges, precoding, control signaling and dynamic SU/MU-MIMO switching.

MU-MIMO combined with a frequency domain packet scheduler for LTE downlink was studied in [5] and it was shown that MU-MIMO with precoding always outperforms MU-MIMO without precoding in terms of ergodic capacity. Other benefits offered by different precoding techniques

for 3GPP LTE and beyond can also be found in [6]. In [7], it was shown that the use of opportunistic scheduling as well as deploying more antennas at either the receiver or both the transmitter/receiver provides higher gain in terms of capacity in uplink compared with single antenna at the receiver.

Maximum Sum-Rate (MSR), Maximum Fairness (Max-Min) and Proportional Fair (PF) scheduling algorithms were investigated in [8], and it was shown that from the physical layer point of view, the MSR performs best in terms of throughput both Max-Min and PF while it is not the case from the Medium Access Control (MAC) where the PF offers the best performance. The results found in [9] show that the SU-MIMO and MU-MIMO cell throughput depends on the antenna configurations at the BS as well as on the antenna spacing. The PF and Max-Rate scheduling algorithms with joint optimization proposed in [10] offered the same performance in terms of bit rate as a function of number of users, and found performance gains with respect to sequential optimization.

It was later shown in [11], that the Exponential/Proportional Fair (EXP/PF) scheduling algorithm outperforms PF, Max-Rate, and Round-Robin scheduling algorithms in terms of system throughput. The scheduling algorithms proposed in [12] for both single-cell and multi-cell MU-MIMO to mitigate both intra-cell and inter-cell interference by the so-called optimal user pairing have shown to offer significant improvement in terms of both cell average user throughput and cell-edge user throughput. To meet the quality of service (QoS) requirements of the real-time traffic such as Voice over Internet Protocol (VoIP) and Video flows, the modified scheduler based on PF, Modified Largest Weighted Delay First (M-LWDF), VT-M-LWDF, Queue-HOL-MLWDF schedulers has been suggested and it has proved to offer best performance in terms of throughput and packet loss ratio (PLR) [13]. In [14], the PF scheduler functionality has been enhanced by proposing a method of predicting future Channel Quality Indicator (CQI) values for high mobility users based on the user's locations. A comparison analysis of different scheduling algorithms in LTE such as Round Robin, Proportional Fair, Best CQI, Resource Fair and Max-Min can be found in [15].

1.5. Limitations

This thesis work has the following limitations:

- SRS bandwidth: Sub-band SRS (24 x 4 PRBs). Due to limitations in the simulator, we cannot consider sub-bands SRS.
- MU-MIMO results for 1SRSAS UE and 1SRSWOAS UE Antenna configurations and different periodicities are not included due to time limitation.

1.6. Thesis outline

This thesis work is organized into 6 chapters. Chapter 1 is an introduction. Chapter 2 reviews the general theoretical background including 3GPP standards, MU-MIMO and scheduling in LTE. Chapter 3 briefly discusses the simulation framework for the scheduler algorithms (SU-MIMO/MU-MIMO). Chapter 4 highlights the obtained results followed by a discussion. Chapter 5 summarizes the main conclusions based on the obtained results. Finally, Chapter 6 includes the future work related to the project work.

2. Background Theory

MIMO antenna system configurations have shown to offer benefits in terms of diversity gain, array gain (beamforming), and spatial multiplexing gain as shown in Fig. 2.1 [16].

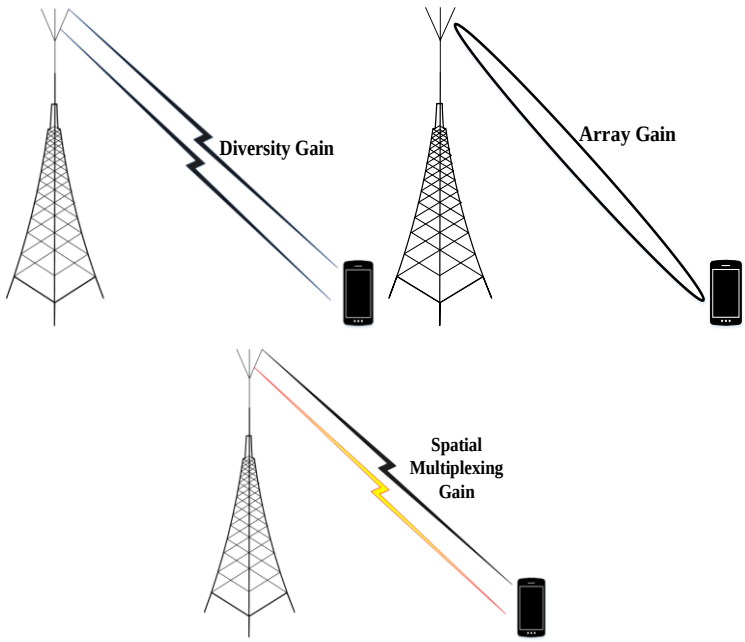

Figure 2.1: Benefits of MIMO [16]

Diversity overcomes fading by using multiple antennas at the receiver (receive diversity) or at the transmitter (transmit diversity) to combine coherently different fading signal paths.

Beamforming increases the received SINR by using multiple antenna elements (antenna arrays) at the transmitter to focus the transmitted energy towards the receiver. Receiver side beamforming is also possible.

Spatial Multiplexing increases the data rate by using multiple antennas at both the transmitter and the receiver such that multiple data streams are transmitted over parallel channels.

To reap the benefits of MIMO, recent 3GPP standards define novel transceiver architectures that support multi-antenna techniques. We describe these architectures below.

2.1. The 3GPP standards

Fig. 2.2 shows the generic block diagram for the downlink physical channel processing [17].

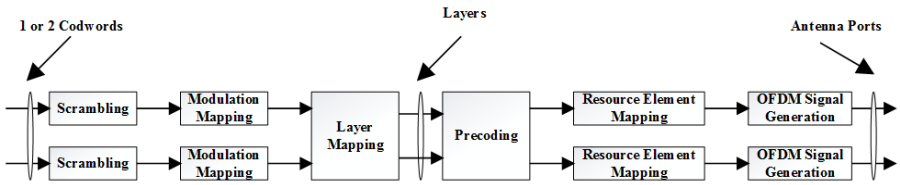

Figure 2.2: Downlink physical channel processing [17]

- Scrambling: Coded bits in each of the codewords to be transmitted on a physical channel are scrambled.
- Modulation/Layer mapping: Scrambled bits are modulated (QPSK, 16QAM, 64QAM, 256QAM) to produce complex symbols and these are mapped onto one or several transmission layers.
- Precoding: Complex symbols are for transmission on the antenna ports.
- Resource element mapping: Precoded complex symbols at each antenna port are mapped to resource elements.
- OFDM signal generation: OFDM symbols for each antenna port are generated.

Codewords in Fig. 2.2 are generated through the following steps [18]:

- Transport block CRC attachment
- Code block segmentation and code block CRC attachment
- Channel coding (Turbo coding)
- Rate matching
- Code block concatenation

Fig. 2.3 shows the general structure for uplink physical channel processing [17].

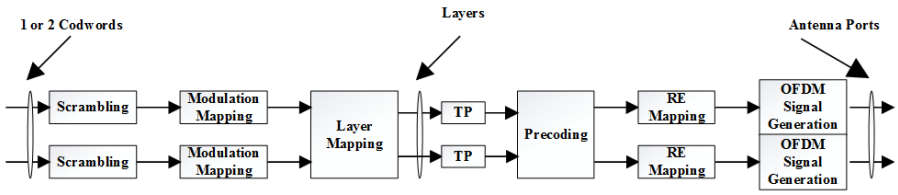

Figure 2.3: Uplink physical channel processing [17]

- Scrambling: Coded bits in each of the codewords to be transmitted on a physical channel are scrambled.
- Modulation/Layer mapping: Scrambled bits are modulated (QPSK, 16QAM, 64QAM) to produce complex symbols and these are mapped onto one or several transmission layers.
- Transform precoding (TP)/Precoding: Complex symbols are precoded on each layer for transmission on the antenna ports after transform precoding.
- Resource element (RE) mapping/SC-FDMA generation: Precoded complex symbols are mapped to resource elements and SC-FDMA symbols for each antenna port are generated.

Codewords in Fig. 2.3 are generated according to [18] through the following steps:

- Transport block CRC attachment
- Code block segmentation and code block CRC attachment
- Channel coding of UL-SCH
- Rate matching
- Code block concatenation and channel coding (Turbo coding)
- Data and control multiplexing
- Channel interleaver.

2.1.1. Frame structure

3GPP defines three radio frame structures of 10 ms duration (each radio frame) as follows [16], [17]:

- Type 1 used in Frequency Division Duplex (FDD) mode only.
- Type 2 used in Time Division Duplex (TDD) mode only.

- Type 3 used in Licensed Assisted Access (LAA) secondary cell operation only.

In this thesis work, only frame structure type 2 is considered. In TDD mode, both uplink and downlink transmissions occur in the same frequency band but at different time periods. Frame structure type 2 is illustrated in Fig. 2.4.

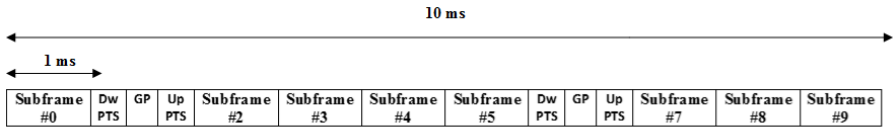

Figure 2.4: Frame structure type 2 (switch-point periodicity = 5ms) [17]

Each radio frame duration (T_f) is 10 ms long and consists of 2 half-frames of length equal to 5 ms (each half-frame). Each half-frame consists of 5 subframes of length equal to 1 ms each. Thus, one radio frame is made up of 10 consecutive subframes numbered from 0 to 9.

Frame structure type 2 defines a special subframe for downlink-to-uplink switch, which comes in two periodicities: 5 ms and 10 ms. With 5 ms downlink-to-uplink switch-point periodicity, the special subframe occurs in both half-frames; with 10 ms downlink-to-uplink switch-point periodicity, the special subframe occurs in the first half-frame only. Subframes zero, five and the downlink part of special subframe (DwPTS) are always associated with downlink transmissions, while the Uplink part of special subframe (UpPTS) and the subframe immediately succeeding the special subframe are always associated with uplink transmissions. GP denotes the guard period between DwPTS and UpPTS.

From the above rules, many uplink-downlink configurations for radio frame type 2 are possible. These are listed in Appendix 2.A, where "D" denotes a subframe associated with downlink transmissions, "U" a subframe associated with uplink transmissions, and "S" a special subframe containing the three parts: DwPTS, GP and UpPTS discussed above [17]. In this thesis work, we are solely concerned with uplink-downlink configuration 2 (see Appendix 2.A).

2.1.2. Physical resource block

A physical resource block (PRB) is the smallest unit of resources that can be allocated to one UE, and extends in both time and frequency domains.

Three different types of PRBs have been defined by 3GPP [16], [17]:

- Normal cyclic prefix with 15 kHz subcarriers.
- Extended cyclic prefix with 15 kHz subcarriers.
- Extended cyclic prefix with 7.5 kHz subcarriers.

In this thesis work, only normal cyclic prefix-PRBs are considered. One such PRB is shown in Fig. 2.5.

The role of the e-Node B's scheduler is to allocate PRBs to the UEs to allow both uplink and downlink data transmissions. The physical resource block structure (Fig. 2.5) is defined as follows [16], [17], [20], [21], [22]: A physical resource block (0.5 ms long in time-domain) contains 7 OFDM symbols in the time domain and 12 subcarriers (180 kHz) in the frequency domain for normal cyclic prefix. As shown in Fig. 2.5, one subcarrier occupies a bandwidth of 15 kHz.

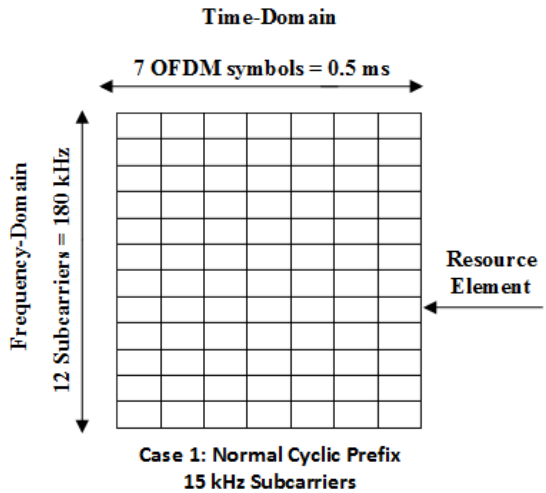

Figure 2.5: Physical resource block (Normal cyclic prefix) [16]

The relationship between the number of physical resource blocks in the frequency-domain and the system bandwidth assuming the subcarrier spacing (Δf) of 15 kHz is shown in Table 2.1 [16].

System bandwidth	= Number of subcarriers x subcarrier spacing
PRB bandwidth	= 12 subcarriers x subcarrier spacing = 180 kHz
Number of PRBs	= System bandwidth / PRB bandwidth

This means that there are 6, 15, 25, 50, 75 and 100 PRBs for 1.4, 3, 5, 10, 15 and 20 MHz system bandwidths respectively.

Table 2.1: Physical resource blocks vs system bandwidth [16]

System bandwidth (MHz)	1.4	3	5	10	15	20
PRBs (Frequency-domain)	6	15	25	50	75	100

2.1.3. Concept of antenna ports in LTE (Downlink)

3GPP introduced the concept of antenna ports in downlink (e-Node B to UE) where one resource grid per antenna port is used and the antenna ports are determined by the reference signal configuration in the cell [17].

Table 2.2 summarizes the different antenna ports configuration with their corresponding supported reference signals [17]:

- Cell-specific reference signals (CRS) are sent on antenna port(s) 0, {0,1} and {0,1,2,3}.
- Downlink demodulation reference signals (DM-$RS_{(DL)}$), sometimes referred to as UE-specific reference signals associated with physical downlink shared channel (PDSCH), are sent on antenna port(s) 5, 7, 8, 11, 13, {11,13} or {7,8,9,10,11,12,13,14}.

Table 2.2: Antenna ports and their respective downlink reference signals [17]

Antenna port(s)	0	{0-1}	{0-3}	5,7,8,11,13	{11,13}	{7-14}
Reference signals	CRS			UE-specific reference signals (DM-$RS_{(DL)}$)		

In this thesis work, antenna ports {0,1} are considered for CRS while for UE-specific reference signals, antenna ports {7,8}. Next we show the resources grids associated with these antenna ports.

Fig. 2.6 illustrates the resource grid of CRS reference signals transmitted on antenna ports $p \in \{0,1\}$ where R_p denotes a resource element corresponding to antenna port p.

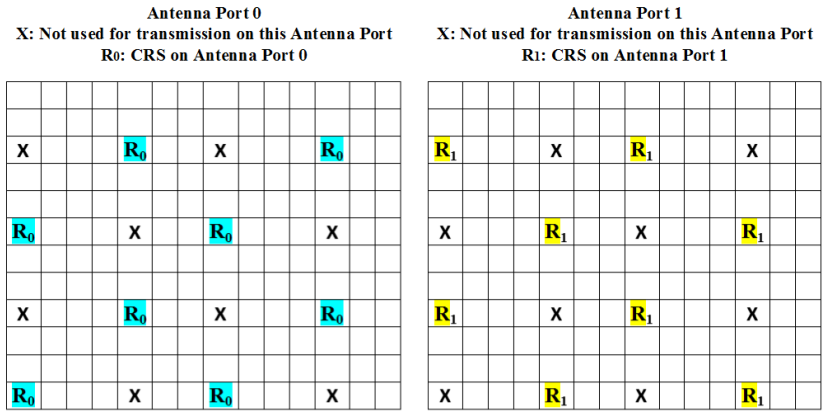

Figure 2.6: Two-antenna port configuration for CRS (Normal cyclic prefix) [17]

Fig. 2.7 illustrates the resource grid of UE-specific reference signals ($\text{DM-RS}_{(\text{DL})}$), transmitted on antenna ports $p \in \{7,8\}$ where R_p denotes a resource element corresponding to antenna port p.

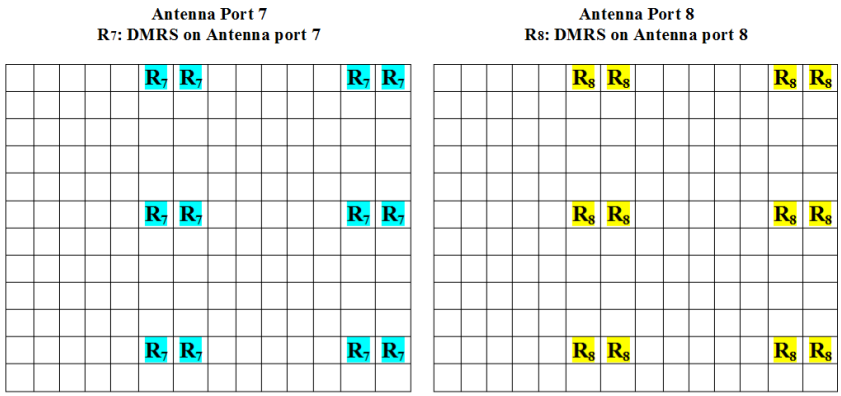

Figure 2.7: Antenna port configuration for UE-specific reference signals, antenna ports 7 and 8 (Normal cyclic prefix) [17]

2.1.4. Concept of antenna ports in LTE (Uplink)

Like the downlink case (see Section 2.1.3), 3GPP introduced also the concept of antenna ports in uplink (UE to e-Node B) where one resource grid per antenna port is used. The antenna ports that are used for

transmission of physical channel or signal are determined by the number of antenna ports as shown in Table 2.3 where [17]:

- The physical uplink shared channel (PUSCH) and SRS use the same antenna ports 10, {20,21} and {40,41,42,43}.
- The physical uplink control channel (PUCCH) and uplink demodulation reference signals (DM-RS$_{(UL)}$) use antenna ports 100 and {200,201}.

Table 2.3: Antenna ports for different physical channels and signals [17]

Antenna port(s)	10	{20,21}	{40-43}	100	{200-201}
Physical channel or signal	PUSCH/SRS			PUCCH/DM-RS$_{(UL)}$	

In this thesis work, antenna ports 10 and {20-21} are considered for PUSCH/SRS while for PUCCH/DM-RS$_{(UL)}$, antenna ports 100, {200-201}.

Fig. 2.8 illustrates the DM-RS$_{(UL)}$ structure (Normal cyclic prefix), sent in each uplink slot (fourth symbol).

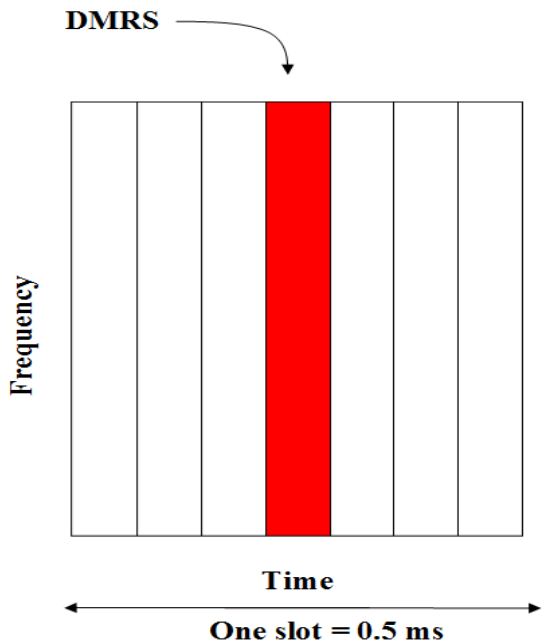

Figure 2.8: DM-RS$_{(UL)}$ structure (Normal cyclic prefix) [16], [20], [21], [22]

With frame structure type 2 (TDD), SRS sequences are sent in uplink subframes, or in special subframes (uplink part). SRS configurations are

defined for full bandwidth (Non-frequency hopping SRS), or for sub-bands (Frequency hopping SRS), as shown in Fig. 2.9 - 2.10 [16], [20], [21], [22].

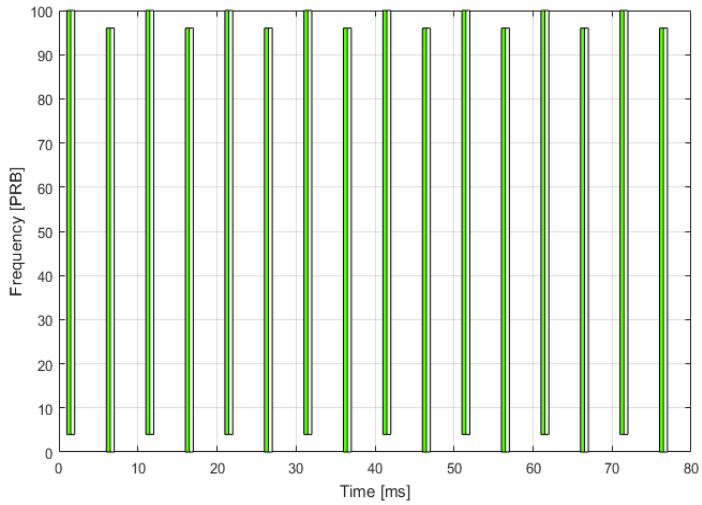

Figure 2.9: Full bandwidth (96 PRBs) SRS configuration and 5 ms SRS (sounding) periodicity

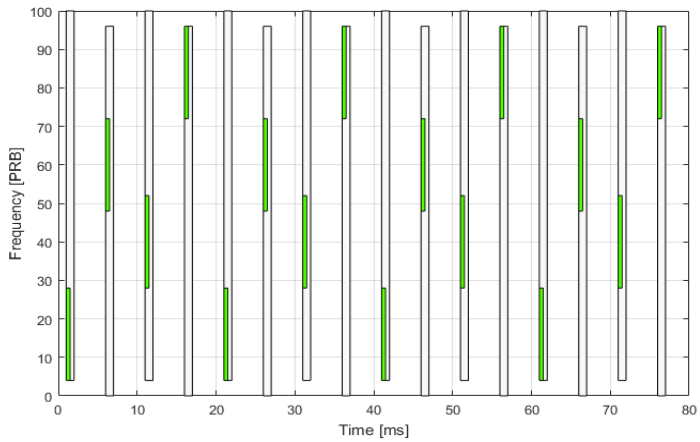

Figure 2.10: Sub-bands (24 PRBs) SRS configuration and 5 ms SRS (sounding) periodicity

2.1.5. Transmission modes in LTE

Different downlink transmission modes (1 to 10) are specified by 3GPP for LTE [19]. In this thesis work, only transmission mode 8 (TM-8), based on dual layer transmission using ports 7 and 8, is considered; see Table 2.4.

TM-8 supports beamforming. In TDD operation, the e-Node B computes the beamforming weights from the SRS by exploiting channel reciprocity [16].

Table 2.4: Transmission mode 8 [19]

Transmission mode	**Transmission scheme of PDSCH**
TM-8	Single-antenna port, port 0 or Transmit diversity (DCI Format 1A)
	Dual layer transmission, ports 7 and 8 or Single-antenna port, port 7 or 8 (DCI Format 2B)

TM-8 in LTE downlink is described in detail in Appendix 2.B. For the uplink case, the different transmission modes (mode 1 and mode 2) specified by 3GPP are given in Table 2.5 [19].

Table 2.5: Basic PUSCH transmission modes [19]

Transmission mode	**Transmission scheme of PUSCH**
Mode 1	Single-antenna port, port 10
Mode 2	Single-antenna port, port 10
	Closed-loop spatial multiplexing

2.1.6. Beamforming

As mentioned at the beginning of Sec. 2, transmitter-side beamforming increases the received SINR by using multiple antenna elements at the transmitter to focus the transmitted energy towards the receiver.

In Fig. 2.11, an e-Node B uses an antenna array to “beamform” transmissions to specific UEs [16].

A description of antenna array configurations used in the simulations can be found in Sec 3.4.

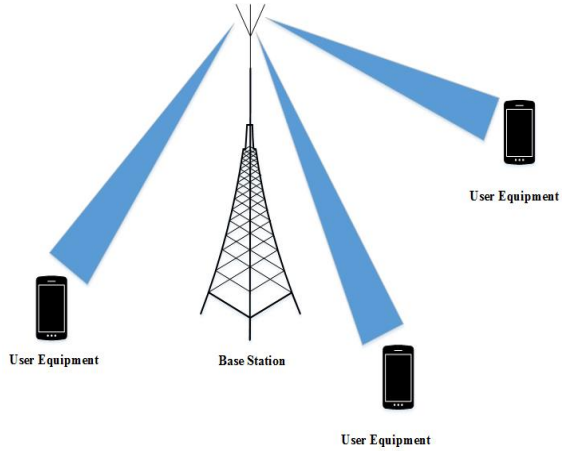

Figure 2.11: Illustration of beamforming (BS side) [16]

2.2. Multi-user Multiple Input Multiple Output (MU-MIMO)

The main difference between SU-MIMO and MU-MIMO is illustrated in Fig. 2.13-2.14. In SU-MIMO, time-frequency resource is allocated to a single user communicating with the e-Node B. In MU-MIMO, different UEs can communicate with the e-Node B using the same time-frequency resource by the so-called spatial separation [1].

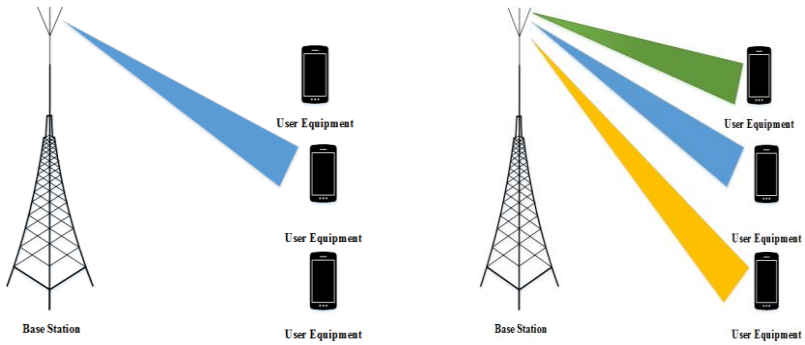

Figure 2.12: Illustartion of SU-MIMO (left), and MU-MIMO (right) [1]

With MU-MIMO, several users can communicate with the BS in the same time-frequency resource.

2.2.1. System model

A general downlink MU-MIMO system is shown in Fig. 2.15 having a BS (e-Node B) equipped with M_T antennas and K UEs each equipped with M_R antennas (usually 1 or 2) in a cell. For the sake of argument, we let M_R = 1 below.

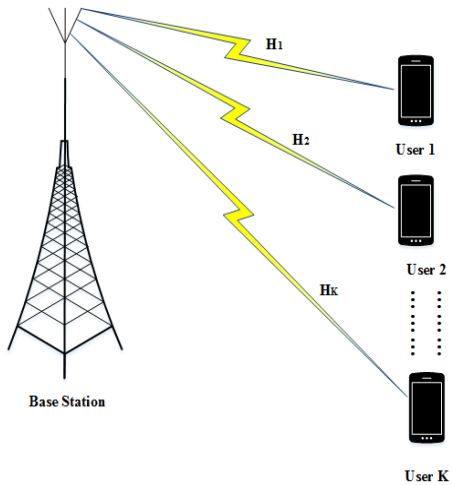

Figure 2.13: System model

We assume a frequency flat channel given by the $K \times M_T$ channel matrix $H = [h_1^T \dots h_K^T]^T$, where h_k is the $1 \times M_T$ MISO channel of user k. The input-output relation of the MU-MIMO channel is given by [26]:

$$y = \sqrt{E_s}Hs + n, (2.1)$$

Where s is the $M_T \times 1$ vector of precoded transmitted symbols satisfying $E\{s^H s\} = 1$, y the $K \times 1$ vector of symbols received by the UEs, n a $K \times 1$ UE noise vector with zero-mean circularly symmetric complex Gaussian (ZMCSCG) independent entries with variance N_0, and E_s is the total average energy available at the BS in one symbol period.

Linear precoding is sometimes assumed, both for its effectiveness and analytical simplicity. With linear precoding at the BS, s takes on the form:

$$s = Wx, (2.2)$$

Where W is a $M_T \times K$ precoding matrix, and $x = [x_1, \dots, x_K]^T$ with x_k the data symbol of user k, which we assume ZMCSCG distributed with unit variance. Inserting (2.2) into (2.1), we obtain:

$$y = \sqrt{E_s}HWx + n, \quad (2.3)$$

Or, using the notation $W = [w_1 \dots w_K]$,

$$y_i = hw_i x_i + h_i \sum_{j=1, j\neq i}^{K} wx_j + n_i, \qquad i = 1, \dots, K. \qquad (2.4)$$

The first part on the right-hand side of equation (2.4) represents the desired received signal at UE i while the middle part represents the multi-user interference (MUI) coming from other UEs in the same cell.

2.2.2. Linear precoding in MU-MIMO

Precoding or pre-filtering at the BS is used to focus the transmitted signal towards the intended users and attempt to null interfering signal towards other users. Pre-filtering methods such as zero forcing (ZF) and minimum mean square error (MMSE) can be found in [26].

The i^{th} column of the ZF pre-filtering matrix, $\mathbf{w}_{ZF,i}$, is given by [26]:

$$W_{ZF,i} = \frac{h_i^{(\dagger)}}{\sqrt{\left\| h_i^{(\dagger)} \right\|_F}} \quad (2.5)$$

where $i = 1, 2, \dots, P$ (P is the number of users), $h_i^{(\dagger)}$ is the i^{th} column of $\mathbf{H}^{\dagger}$, and $E_{s,i}$ is chosen subject to the power constraint $\sum_{i=1}^{P} E_{s,i} = E_s$.

For the MMSE precoder, the SINR at the i^{th} user is given by [26]:

$$SINR_i = \frac{|h_i w_i|^2 E_{s,i}}{\left(\sum_{j=1, j\neq i}^{P} |h_i w_i|^2 E_{s,i}\right) + N_0} \quad (2.6)$$

where $i = 1, 2, \dots, P$ (P is the number of users), $\mathbf{h}_i$ is the i^{th} row of $\mathbf{H}$, and $E_{s,i}$ is chosen subject to the power constraint $\sum_{i=1}^{P} E_{s,i} = E_s$ and $\|w_i\|^2{}_F = 1$.

The drawbacks of a ZF precoder are power reduction and noise enhancement problems. However, MMSE precoder outperforms ZF precoder by trading interference reduction for signal power inefficiency.

2.3. Scheduling in LTE

The main task of the scheduler is to determine how the shared time-frequency resources should be allocated to different UEs. To accomplish this task, both uplink and downlink schedulers are implemented in the e-Node B. The scheduling decisions are often taken every Transmission Time Interval (TTI), i.e. one millisecond [20], [21], [22].

- The downlink scheduler determines which UEs upon which the DL-SCH should be transmitted by assigning time-frequency resources to them.
- The uplink scheduler determines which UEs should transmit on their UL-SCH by assigning time-frequency resources to them.

2.3.1. Scheduling strategies

Different scheduling strategies such as Max-C/I (or maximum rate), Round Robin (RR) and Proportional Fair (PF) have been briefly discussed in [20], [21], [22]. In this thesis work, only the RR scheduler is considered. Its principle is based on assigning time-frequency resources to different UEs in a cyclic fashion for the same amount of time without considering the channel conditions experienced by different UEs [20], [21], [22].

2.3.2. Downlink packet scheduling in LTE

As mentioned earlier, the uplink and downlink schedulers are in the e-Node B. Scheduling decisions are taken every TTI (1 ms) by allocating time-frequency resources to different UEs. These resources are in the data region while the downlink and uplink scheduling information is in the control region of the downlink subframe. Within 1 ms, the control region occupies 1 to 4 OFDM symbols (usually 3) which is indicated by the Physical Control Format Indicator Channel (PCFICH) and the data region where the Physical Downlink Shared Channel (PDSCH) is located, occupies the remaining OFDM symbols (usually 11), as shown in Fig. 2.14 [27].

Control Region: 3 OFDM signals dedicated to signaling information

Data Region: Remaining 11 OFDM signals used for data transmission

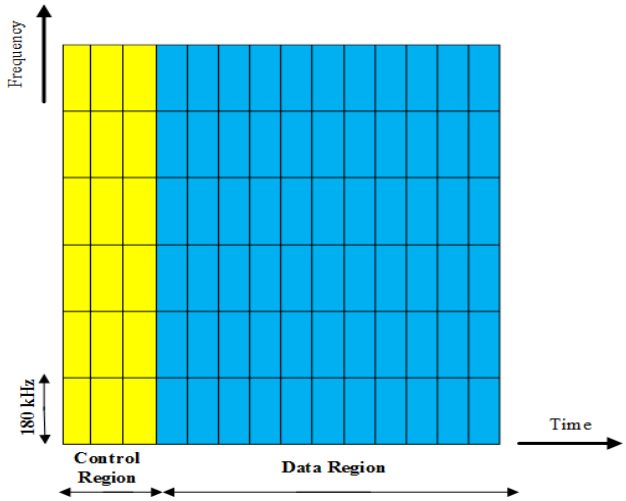

Figure 2.14: Time-Frequency structure of the LTE downlink subframe (example with 3 OFDM symbols dedicated to control channels) [27]

The control region contains the following downlink physical channels: Physical Control Format Indicator Channel (PCFICH), Physical Hybrid-ARQ Indicator Channel (PHICH) and Physical Downlink Control Channel (PDCCH), while in the data region, there are: Physical Downlink Shared Channel (PDSCH) and Physical Broadcast Channel (PBCH) [28].

From scheduling point of view, the PDCCH and PDSCH are the ones of main interest. The PDCCH carries the downlink control information (DCI) indicating where the downlink (DL) and uplink (UL) scheduling information is located. This DCI message informs UE devices where to find their data on the PDSCH [27], [28]. Different DCI formats used for scheduling and power control purposes are listed in Table 2.6. In this thesis work, DCI format 2B is the one which will be considered. It is associated with transmission mode 8 (TM-8) and used for scheduling with dual layer transmission as shown in Table 2.6.

Table 2.6: Supported DCI formats in REL. 8–11 [28]

DCI Formats		Purpose
UL Scheduling (PUSCH)	**0**	UL Scheduling + TPC (PUSCH)
	4	UL Scheduling with **CLSM** + TPC (PUSCH) (Rel. 10-11)
DL Scheduling (PDSCH)	**1**	Scheduling, TPC (PUCCH)
	1A	**Compact** Scheduling with **TxD**, TPC (PUCCH)
	1B	**Compact** Scheduling with **CLSM**, TPC (PUCCH)
	1C	**Very Compact** Scheduling
	1D	**Compact** Scheduling with **MU-MIMO**, TPC (PUCCH)
	2	Scheduling with **CLSM or TxD**, TPC (PUCCH)
	2A	Scheduling with **Large CDD or TxD**, TPC (PUCCH)
	2B	Scheduling with **Dual Layer Transmission**, TPC (PUCCH) (Rel. 9-11)
	2C	**Up to 8 Layered Compact** Scheduling, TPC (PUCCH) (Rel. 10-11)
	2D	**Up to 8 Layered Compact** Scheduling for **CoMP**, TPC (PUCCH) (Re. 11)
UL Power Control	**3**	TPC for PUCCH, PUSCH 2bit Power Adjustment
	3A	TPC for PUCCH, PUSCH 1bit Power Adjustment

In Table 2.6, we have used the following abbreviations:

TPC: Transmit Power Control

CLSM: Closed Loop Spatial Multiplexing

TxD: Transmit Diversity

MU-MIMO: Multi-User MIMO

CDD: Cyclic Delay Diversity

CoMP: Co-ordinated Multi Point

2.3.3. Downlink (DL) resource allocation

Three types of DL resource allocation supported by LTE are defined [28]: Type 0, Type 1, and Type 2; but only Type 0 will be considered in this thesis work. DL resource allocation Type 0's bits and associated DCI formats are given in Table 2.7. Type 0 is indicated by setting the "resource allocation header" field to 0.

The number of resources to be allocated in downlink within a subframe (or TTI = 1 ms) is given by [28]:

$$RA = \frac{N_{RB}^{DL}}{P},$$

Where RA denotes the Resource Assignment, N_{RB}^{DL} is the system bandwidth (BW) in terms physical resource blocks (PRBs) available in downlink, P is the resource block group (RBG) size.

Table 2.7: DL resource allocation Type 0 with DCI formats 2/2A/2B/2C/2D [28]

Bits	**DCI format 2/2A/2B*/2C*/2D***
0 to 3	**Carrier Indicator in Rel. 10-11**
1	**Resource allocation header:** Set to **0**
$\left\lceil \frac{N_{RB}^{DL}}{P} \right\rceil$	**Resource Allocation Type 0** $\left\lceil \frac{N_{RB}^{DL}}{P} \right\rceil$: Resource Assignment
2	**UL Power Control** (PUCCH)
2	**Downlink Assignment Index** (TDD DL/UL Configuration 1-6)
3 or 4	**HARQ process number:** 3 bits (FDD), 4 bits (TDD)
1 or 3	**1 bit:** Codeword Swap Flag or Scrambling Identity **3 bits:** Antenna port(s), Scrambling Identity, # layer in Rel. 10-11
0 or 1	**SRS Request** only for TDD mode in Rel. 10-11
8+8	**For transport block 1 & 2:** 5 bits (MCS) + 1 bit (New data indicator) + 2 bits (Redundancy version)
0, 2, 3, 6	**DCI Format 2 Closed Loop MIMO:** 3 (# Ant. ports 2), 6 (# Ant. ports 4) **DCI Format 2A Open Loop MIMO:** 0 (# Ant. ports 2), 2 (# Ant. ports 4)
2	**DCI Format 2D*:** PDSCH RE Mapping and Quasi-Co-Location Indicator
2	**HARQ-ACK resource offset only for EPDCCH in Re. 11**

As shown in Fig. 2.15, P is uniquely determined by N_{RB}^{DL}. Up to 25 RBGs (numbered from RBG 0 to RBG 24) are allocated in downlink within a system bandwidth of 100 MHz where each RBG is equal to 4 PRBs as indicated by the parameter P. P = 4 in this case [28]. Within 100 MHz, there are 100 PRBs with each PRB having 12 subcarriers (180 kHz) in 0.5 ms.

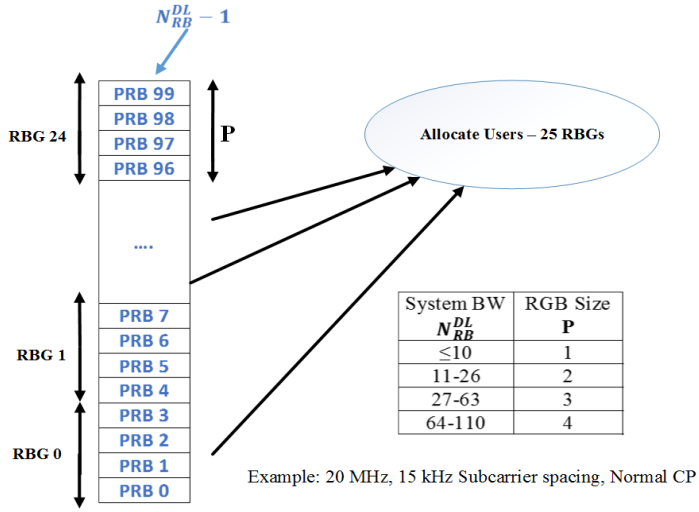

Figure 2.15: DL resource allocation type 0 [28]

Fig. 2.16 illustrates DL SU-MIMO scheduling and DL MU-MIMO scheduling (Resource Allocation Type 0 for 3 UEs: UE1, UE2 & UE3) with the following examples:

- Full-Buffer (FB) traffic: In SU-MIMO, 25 RBGs are allocated to each UE every TTI, while in MU-MIMO, 3 users are paired (co-scheduled) and allocated same 25 RBGs. In FB traffic case, UEs send or receive data all time.
- File Transfer Protocol (FTP) traffic: In SU-MIMO, UE1 needs 4 RBGs, UE2 needs 3 RBGs and UE3 needs 2 RBGs in 1 TTI, while in MU-MIMO, UE1 needs 4 RBGs, UE2 needs 7 RBGs and UE3 needs 9 RBGs because of MU-pairing in 1 TTI. In FTP traffic case, UEs send or receive according to their buffer size status, e.g. 1 kB, 10 kB, 100 kB, 1 MB and so on.

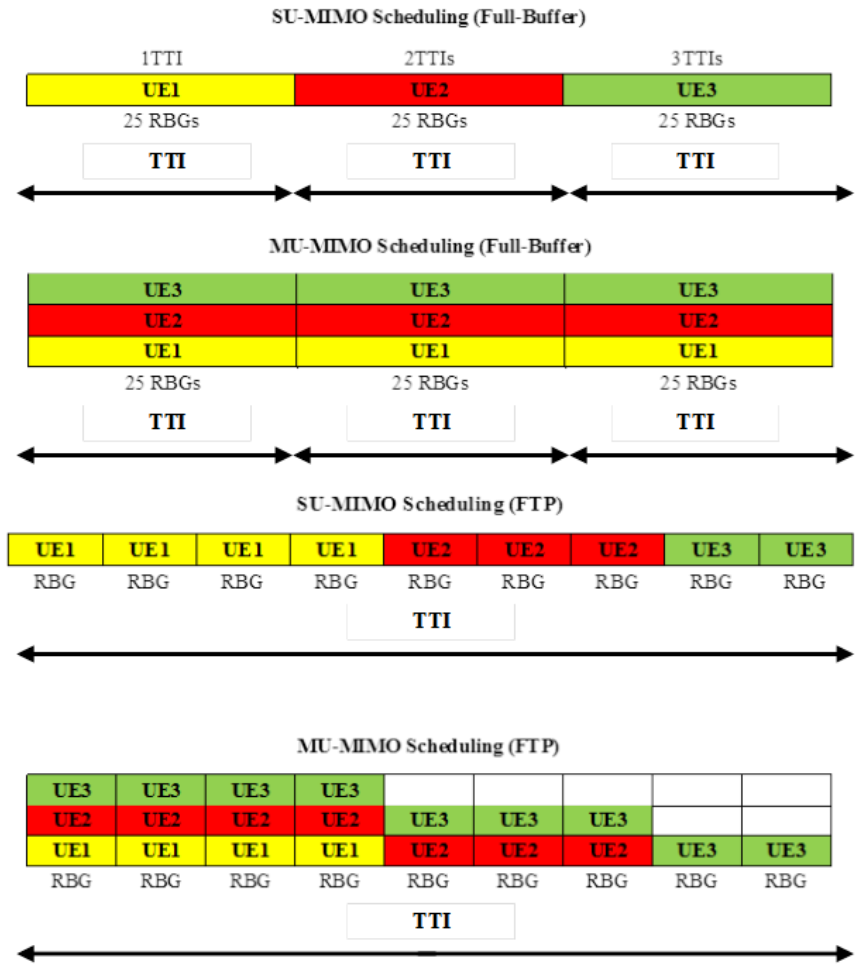

Figure 2.16: DL SU-MIMO scheduling vs DL MU-MIMO scheduling

3. Simulation Framework

In this thesis work, the performance evaluation is based on system level simulations. The simulation framework is organized according to Fig. 3.1.

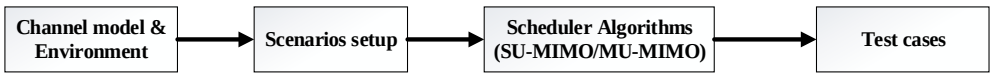

Figure 3.1: Simulation framework

- Channel model and environment: Spatial channel models (SCM) and urban macro environment are considered (see Section 3.1).
- Scenario setup: Scenarios setup includes the system cell deployment and system configurations parameters (see Section 3.2).
- Scheduler algorithms for SU/MU-MIMO: Scheduler algorithms for SU/MU-MIMO are based on precoding considering ICI, and without considering ICI (see Section 3.3).
- Test cases: Test cases are based on different parameters (see Section 3.4).

3.1. Channel model and environment

In this section, the spatial channel model (SCM) and the urban macro (UMa) environment are succinctly described.

3.1.1. Channel model

For simulation purposes in this thesis work, we use the 3GPP SCM channel model described in [23], [24], [25]. Two types of SCM are considered:

- Two dimensional (2D) SCM [25]
- Three dimensional (3D) SCM [23], [24]

The main 2D SCM parameters at both the base station (BS) side and mobile station (MS) side are given in Table 3.1.

Table 3.1: 2D SCM parameters [25]

Parameters	**Antenna pattern per sector (dB)**	**Power Azimuth Spectrum (PAS) per-path**
BS side	$A(\theta) = -min\left[12\left(\frac{\theta}{\theta_{3dB}}\right)^2, A_m\right]$	$P(\theta,\sigma,\bar{\theta}) = N_0 exp\left[\frac{-\sqrt{2}\lvert\theta-\bar{\theta}\rvert}{\sigma}\right] G(\theta)$
MS side	-1 dBi (Omni-directional)	$P(\theta,\sigma',\bar{\theta}') = N_0 exp\left[\frac{-\sqrt{2}\lvert\theta-\bar{\theta}'\rvert}{\sigma'}\right]$

Where:

- θ: -180 degrees ≤ θ ≤ +180 degrees
- θ_{3dB} = 70 degrees (3 sector scenario)
- Am = 20 dB (3 sector scenario)
- N_0: Normalization constant
- $G(\theta)$: BS antenna gain
- $\bar{\theta}$: Angle of departure (AoD) at the BS side
- σ: Root mean-square (RMS) angle-spread (AS) at the BS side
- $\bar{\theta}'$: Angle of arrival (AoA) at the MS side
- σ': Root mean-square (RMS) angle-spread (AS) at the MS side

The main 3D SCM parameters are given in Table 3.2.

Table 3.2: 3D SCM parameters [23], [24]

Parameters	**values**
Antenna element vertical radiation pattern (dB)	$A_{E,V}(\theta'') = -min\left[12\left(\frac{\theta''-90^0}{\theta_{3dB}}\right)^2, SLA_V\right], \theta_{3dB} = 65^0, SLA_V = 30\ dB$
Antenna element horizontal radiation pattern (dB)	$A_{E,H}(\varphi'') = -min\left[12\left(\frac{\varphi''}{\varphi_{3dB}}\right)^2, A_m\right], \varphi_{3dB} = 65^0, A_m = 30\ dB$
3D antenna element pattern (dB)	$A''(\theta'',\varphi'') = -min\{-[A_{E,V}(\theta'') + A_{E,H}(\varphi'')], A_m\}$

3.1.2. Environment

For our performance evaluation, we selected the **"urban macro-cell"** environment of 3GPP SCM [25]. The path-loss (PL) for this environment is given by:

$$PL\ (dB) = A + B + 37.6 \log_{10}(d) \quad (3.1)$$

Where

- A is the attenuation constant (15.3 dB)
- B is the additional loss for indoor mobiles (20 dB)
- d is the distance between BS and MS in meters

Table 3.3: Urban macro cell environment parameters [25]

Parameters	**Value**	
Number of paths (N)	6	
Number of sub-paths (M) per-path	20	
AS at BS (lognormal RV)	15^0	$\mu_{AS} = 1.18$
		$\varepsilon_{AS} = 0.210$
DS, lognormal RV)	0.65 μs (RMS)	$\mu_{DS} = -6.18$
		$\varepsilon_{DS} = 0.18$
Angular spread scaling parameter (r_{AS})	1.3	
Delay spread scaling parameter (r_{DS})	1.7	
Lognormal shadowing standard deviation, σ_{SF}	8 dB	

The main parameters defining the urban macro cell environment are given in Table 3.3, where we have used the following abbreviations:

- DS: Delay spread
- AS: Angular spread
- RMS: Root mean square
- μ_{AS}: mean AS
- ε_{AS}: AS standard deviation
- μ_{DS}: mean DS
- ε_{DS}: DS standard deviation

3.2. Scenario setup

3.2.1. System cell deployment

The system deployment is a 3GPP case 1 (Table 3.4) where the inter-site distance (ISD) is equal to 500 meters [29].

Table 3.4: System cell deployment parameters

Parameters	Value
Cell layout	Hexagonal grid, 7 sites, 3 sectors per site
Inter-site distance (ISD)	500 meters
Carrier frequency	2 GHz
BS Max. Tx Power	40 watts or 46 dBm
Number of users (UEs)	210 (7 sites)/30 per site/10 per sector

3.2.2. System configurations parameters

The main system configuration parameters are given in Table 3.5.

Table 3.5: System configurations parameters

Parameters	Value
System bandwidth	20 MHz (100 PRBs)
Frame structure	Frame type 2 (TDD)
TDD configuration	Uplink-Downlink configuration 2 (see Appendix 2.A)
Transmission Mode	TM-8 (2 layers-transmission & Beamforming)
Scheduler	Round Robin (RR)

3.3. Scheduler algorithms for MU-MIMO

The following steps, illustrated in Fig. 3.2, briefly summarize the two scheduler algorithms for MU-MIMO evaluated in this thesis work. These are algorithm 1, which does not consider ICI, and algorithm 2, which does consider ICI.

Note that, although the processing flow Fig. 3.2 addresses MU-MIMO scheduling only, it can be easily adapted for SU-MIMO scheduling. This can be accomplished by simply ignoring steps 3 and 4 (UEs spatial separation, and MU-MIMO pairing blocks, respectively) whenever with SU-MIMO scheduling is desired.

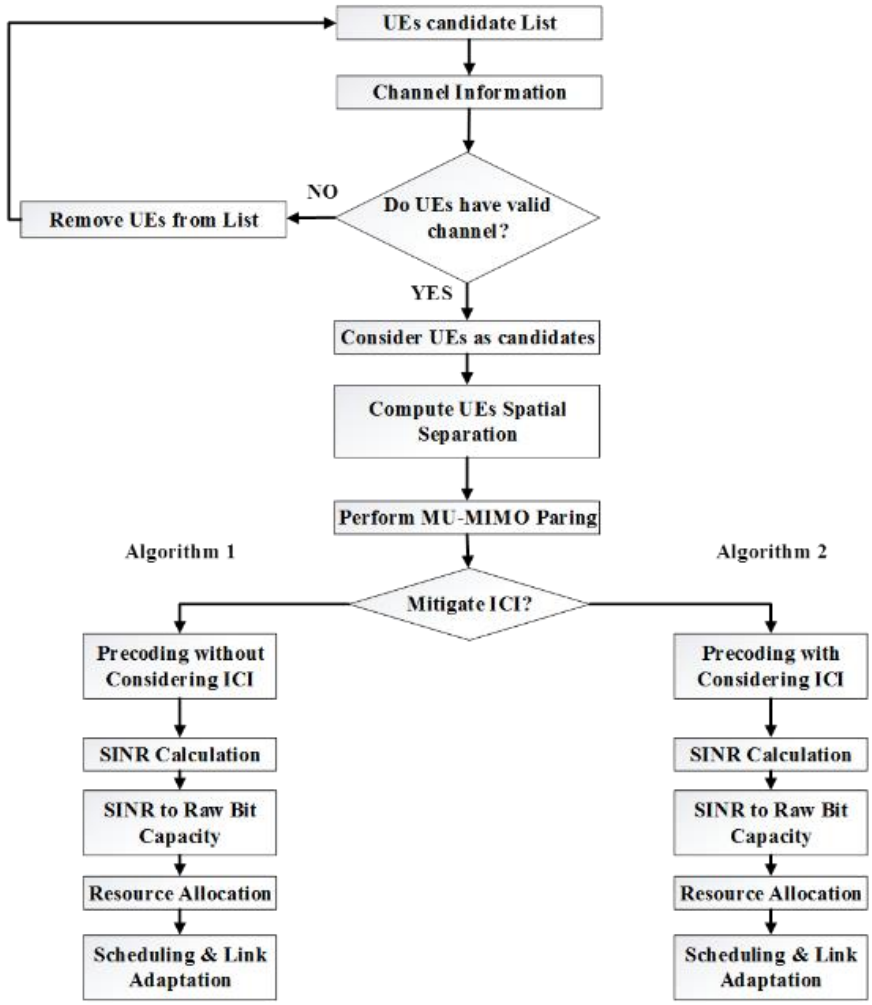

Figure 3.2: Scheduler algorithms for MU-MIMO

Step 1. **UEs candidate list:** The e-Node B creates a list of all candidate UEs to be scheduled in a cell.

Step 2**. Channel information and validation:** The BS acquires the channel information from UE's SRS. For every UE candidate, the BS validates that the channel information stored is not older than the report periodicity value at the scheduling time.

Step 3. **UEs spatial separation:** This operation is based on the UEs channel information, and UEs to be paired must have a sufficiently low

channel correlation (UEs separated in space) according to a certain threshold value, the orthogonality factor (OF).

Step 4. **MU-MIMO pairing:** UEs with sufficiently low channel correlation are the ones to be co-scheduled (paired).

Step 5. **Precoding:** The precoding operations, based on MMSE (see Section 2.2.3), are done differently for the two algorithms, i.e., Algorithm 1 and Algorithm 2.

Step 6. **SINR calculation:** The SINR is calculated based on the precoding.

Step 7. **SINR to raw bit capacity:** This operation maps between the calculated SINR and lookup table to calculate the raw bit capacity.

Step 8**. Resource allocation:** Resources are allocated according to the algorithms introduced to the reader in Section 2.3.3.

Step 9. **Scheduling and link adaptation:** The Scheduler will choose the appropriate modulation and coding scheme (MCS) for this transmission.

3.4. Test cases

The simulated test cases are based on various parameters, including: UEs traffic profile, SRS UL antenna configuration, BS ULA topology, SRS bandwidth and sounding periodicity, and UEs' moving speed. The values taken by these parameters are given in Table 3.6.

Table 3.6: Test cases' parameters

UEs traffic profile	Full-Buffer/FTP		
SRS UL antenna configuration	2SRS UE		
	1SRSAS UE		
	1SRSWOAS UE		
BS ULA topology	1x4x2	4x8x2	
SRS bandwidth	96 PRBs		
SRS periodicity	5 ms	10 ms	20 ms
UEs mobility	3 km/h	30 km/h	60 km/h

The SRS configurations considered, shown in Fig. 3.3, are: (a) Two transmit SRS UE (2SRS UE), (b) one transmitting SRS UE with antenna selection (1SRSAS UE), and (c) one transmitting SRS UE without antenna selection (1SRSWOAS UE).

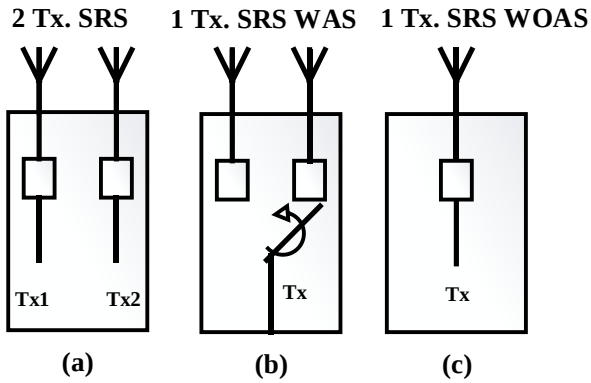

Figure 3.3: (a) 2SRS UE, (b) 1SRSAS UE, (c) 1SRSWOAS UE

For 2SRS UE, two SRS are sent simultaneously to the BS from the two UE's antennas. For 1SRSAS UE, one SRS is sent to the BS from one UE antenna at a given periodicity time, while another SRS is sent to the BS from the other UE antenna at the next periodicity time, using an antenna switch. Thus, for 1SRSAS UE, the actual SRS periodicity is doubled. For 1SRSWOAS UE, one SRS, which correspond to one of the dual layers, is sent to the BS from one UE antenna at each periodicity time, while the other layer information is estimated according to the orthogonality principle at the BS.

The following base station uniform linear array (BSULA) topologies are considered:

- 1x4x2 ULA topology (Fig. 3.4): This topology consists of one row of four cross-polarized antenna elements (i.e. 8 antenna ports) with a horizontal spacing $d_H = 0.5\lambda$ between antenna elements, where λ is the wavelength at the carrier frequency.
- 4x8x2 ULA topology (Fig. 3.5): This topology consists of four rows of eight cross-polarized antenna elements per row (i.e. 64 antenna ports) with a horizontal spacing $d_H = 0.5\lambda$ and a vertical spacing $d_V = 0.7\lambda$ between antenna elements, where λ is the wavelength at the carrier frequency.

Figure 3.4: 1x4x2 ULA topology

Figure 3.5: 4x8x2 ULA topology

4. Results and Discussion

The simulation results are obtained through the following steps, illustrated in Fig. 4.1 by means of a system level simulator:

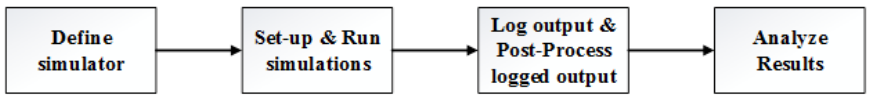

Figure 4.1: Workflow using the system level simulator

- Define simulator: This includes specifying the libraries to be imported by the simulator. For example, radio network functions, protocols, nodes, etc.
- Set-up and run simulations: This includes setting parameter values of the simulator radio network functions, defining traffic load, site deployment, number of iterations (users), etc.
- Log output and post-process logged output: This includes logging the output from the simulation and post-processing of the logged output e.g. by using MATLAB.
- Analyze results: This means evaluating the outcomes form the logged output for different test cases.

  In this chapter, the logged output includes:

- End to End (E2E) average downlink throughput per cell in bits/second.
- User throughput/BW vs. Average served traffic per cell/BW both in bits/second/Hertz.

E2E downlink cell throughput description means serving cell downlink throughput as measured by layer 3 (i.e., it does not include MAC/RLC/HARQ).

All the curves are normalized by using the following same constants: ε (average downlink throughput per cell), and α (UE throughput/BW vs. Average cell throughput/BW).

As we have already mentioned, the algorithms for both SU-MIMO and MU-MIMO are grouped into:

- Algorithm 1: based on precoding without considering ICI (WOCICI).

- Algorithm 2: based on precoding considering ICI (WCICI)

The performance evaluation for both algorithms (SU/MU-MIMO) to be considered is based on the following main test cases' parameters:

- UEs speed
- SRS UL antenna configuration
- SRS parameters (SRS bandwidth/SRS periodicity)
- BS ULA topology

The purpose of this part is not only to evaluate the performance of the system under consideration, but also to verify the correctness of some of the functions in the system simulator, which is still under construction. Indeed, several important bugs were found in various functions and reported to Ericsson AB to be corrected.

The rest of this chapter is structured as follows. In Sec. 4.1, 4.2, and 4.3, we present our results for SU-MIMO with FTP traffic profile and 8 BS antenna elements, SU-MIMO with FB traffic profile and 64 BS antenna elements, and MU-MIMO with FB traffic profile and 64 BS antenna elements, respectively. Then, in Section 4.4 we present a comparative analysis for these three cases.

4.1. SU-MIMO (FTP traffic profile and 8 BS antenna elements)

The main simulation parameters for SU-MIMO with FTP traffic profile and 8 BS antenna elements (BSULA topology: 1x4x2**)** are given in Table 4.1.

Table 4.1: Simulation parameters for SU-MIMO with FTP traffic profile and 8 BS antenna elements (BSULA topology: 1x4x2)

System bandwidth	20MHz
Frame configuration	TDD (2 UL subframes per frame)
Number of DL layers	2
Number of BS antenna elements	8
Beamforming weights	With and without considering ICI
Propagation model	2D SCM urban macro environment
7 sites x 3 sectors	21 cells, 3GPP case 1 (ISD 500m)
SRS (sounding) bandwidth	96 PRBs (Full-bandwidth)
SRS (sounding) periodicity (ms)	[5, 10, 20]
SRS UL antenna configuration	2SRS UE, 1SRSAS UE, 1SRSWOAS UE
UE speed (km/h)	[3, 30, 60]
UE traffic profile	FTP (100 kilobytes), two downloads per UE with mean time between them of 20 ms, then the UE disconnects from the system and a new UE enters after 100 ms.
Scheduling strategy	Round Robin
Seeds	10, 10.005 seconds/seed
Number users as iteration variable	[1,7,14,21,42,63,84,105,210]

4.1.1. SU-MIMO @8 BS antenna elements @5 ms SRS periodicity: 2SRS UE, 1SRSAS UE, 1SRSWOAS UE

Fig. 4.2 (2SRS UE), Fig. 4.3 (1SRSAS UE), and Fig. 4.4 (1SRWOAS UE), illustrate average downlink throughput per cell, SU-MIMO case with 8 BS antenna elements, FTP traffic profile, 5 ms sounding periodicity, and 3, 30 and 60 km/h UE moving speeds.

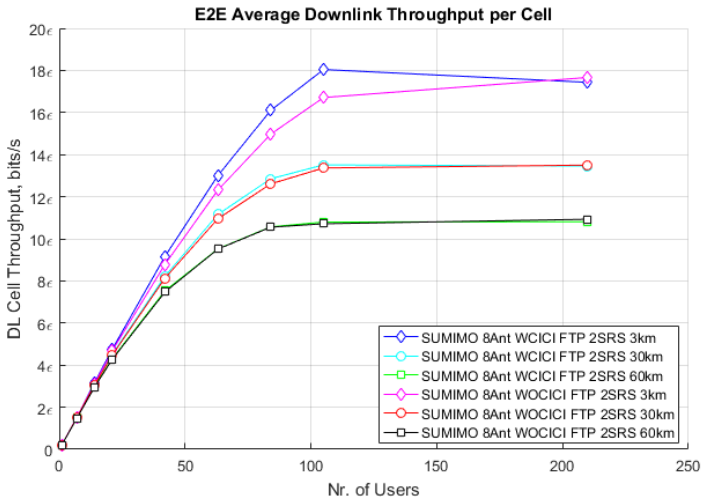

Figure 4.2: Average downlink throughput/cell @SU-MIMO_8 BS antenna elements @2SRS UE @5ms SRS periodicity @FTP

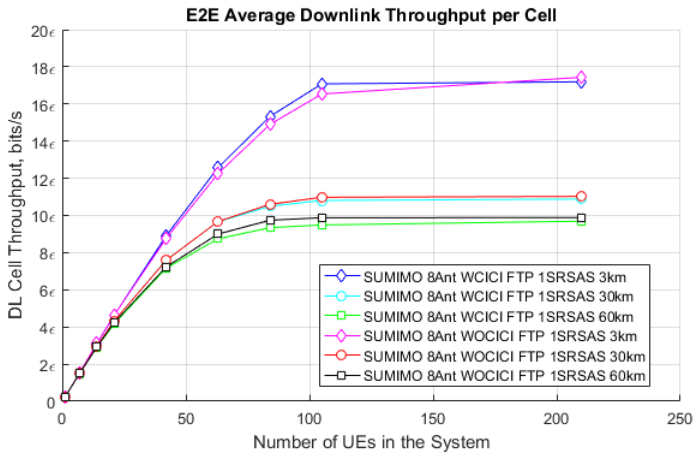

Figure 4.3: Average downlink throughput/cell @SU-MIMO_8 BS antenna elements @1SRSAS UE @5ms SRS periodicity @FTP

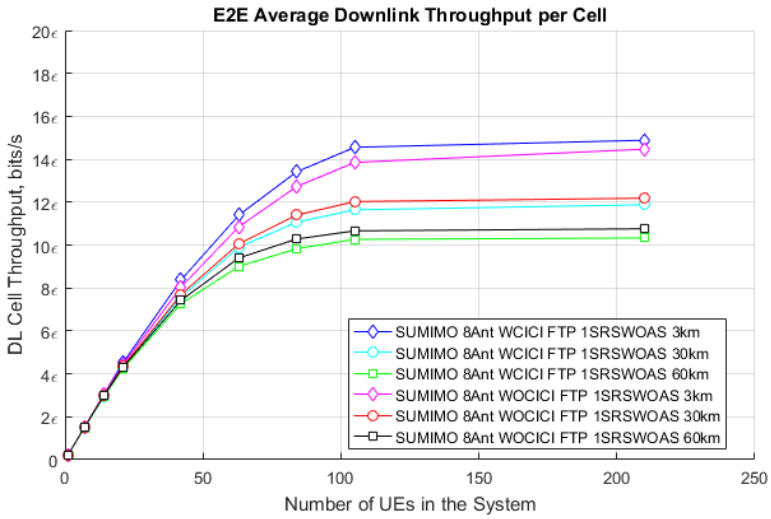

Figure 4.4: Average downlink throughput/cell @SU-MIMO_8 BS antenna elements @1SRSWOAS UE @5ms SRS periodicity @FTP

From Fig. 4.2, Fig 4.3, and Fig. 4.4, the following observations can be made:

- **Fig. 4.2, Fig. 4.3, and Fig. 4.4:** In general, the average downlink throughput per cell decreases with increasing UE speeds for both algorithms (WCICI & WOCICI) and that is because of larger Doppler spreads.
- **Fig. 4.2:** Algorithm 2 (WCICI) outperforms algorithm 1 (WOCICI) in terms of average downlink throughput per cell for 3km/h UE speed. However, for 30 and 60 km/h UE speeds, both algorithms (WCICI & WOCICI) offer almost the same performance.
- **Fig. 4.3:** Both algorithms (WCICI & WOCICI) offer almost the same performance in terms of average downlink throughput per cell for 3 km/h UE speed. However, for 30 and 60 km/h UE speeds, algorithm 1 (WOCICI) outperforms slightly algorithm 2 (WCICI).
- **Fig. 4.4:** Algorithm 2 (WCICI) outperforms algorithm 1 (WOCICI) in terms of average downlink throughput per cell for 3km/h UEs speed. However, for 30 and 60 km/h UE speeds, it is the opposite.

Fig. 4.5 (2SRS UE), Fig. 4.6 (1SRSAS UE), and Fig. 4.7 (1SRSWOAS UE), illustrate User throughput vs. Average served traffic per cell, SU-

MIMO case with 8 BS antenna elements, FTP traffic profile, 5 ms sounding periodicity, and 3, 30 and 60 km/h UE moving speeds.

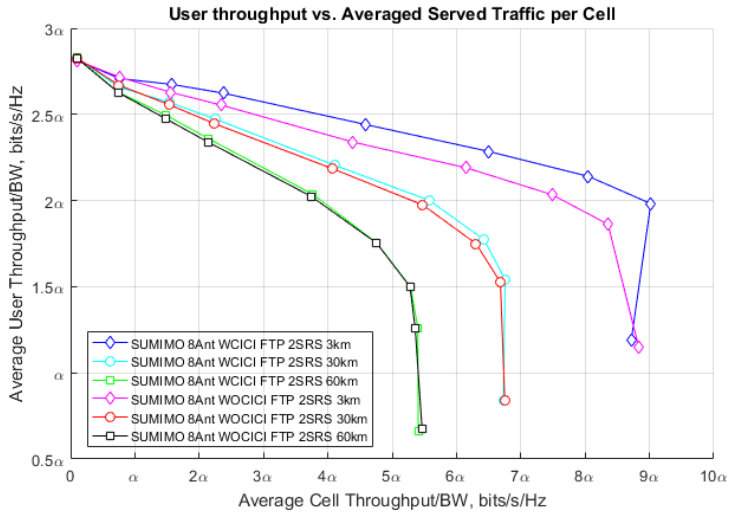

Figure 4.5: User throughput vs. Average served traffic per cell @SU-MIMO_8 BS antenna elements @2SRS UE @5ms SRS periodicity @FTP

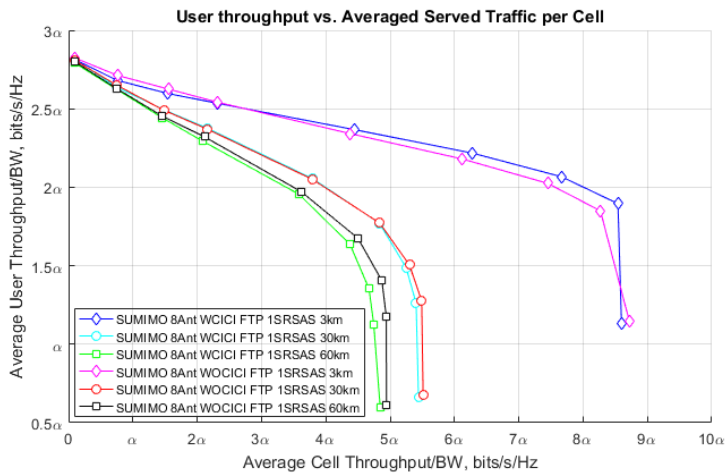

Figure 4.6: User throughput vs. Average served traffic per cell @SU-MIMO_8 BS antenna elements @1SRSAS UE @5ms SRS periodicity @FTP

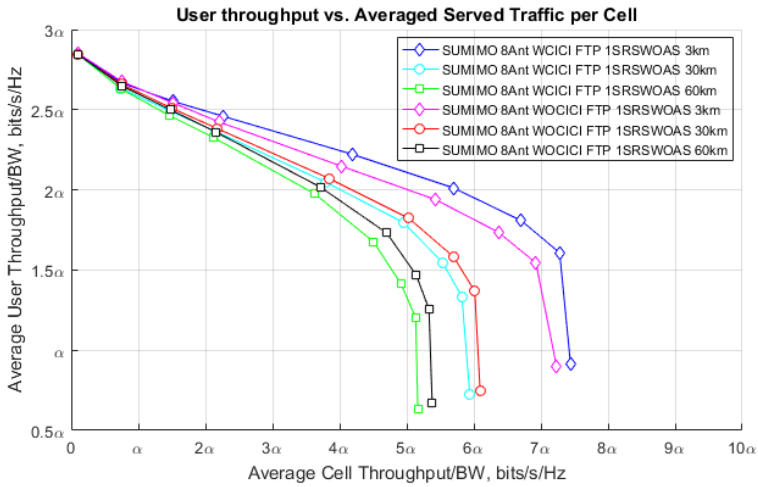

Figure 4.7: User throughput vs. Average served traffic per cell @SU-MIMO_8 BS antenna elements @1SRSWOAS UE @5ms SRS periodicity @FTP

Fig. 4.5, Fig. 4.6, and Fig. 4.7 can be interpreted in the following way:

- **Fig. 4.5, Fig. 4.6, and Fig. 4.7:** The number of UEs to be optimally handled decreases with increasing UE speed for a given user throughput-spectral efficiency threshold for both algorithms (WCICI & WOCICI).
- **Fig. 4.5:** For a user throughput-spectral efficiency threshold of 2α bits/sec/Hz as an example, the system can handle optimally 84 UEs with algorithm 1 (WOCICI) and 105 UEs with algorithm 2 (WCICI) for 3 km/h UE speed, and 63 UEs for 30 km/h UE speed and 42 UEs for 60 km/h UE speed with both algorithms (WCICI & WOCICI).
- **Fig. 4.6:** For a user throughput-spectral efficiency threshold of 2α bits/sec/Hz as an example, the system can handle optimally 84 UEs for 3 km/h UE speed and approximately 42 UEs for 30 and 60 km/h UE speeds with both algorithms (WCICI & WOCICI).
- **Fig. 4.7:** For a user throughput-spectral efficiency threshold of 2α bits/sec/Hz as an example, the system can handle optimally 63 UEs for 3 km/h UE speed and approximately 42 UEs for 30 and 60 km/h UE speed with both algorithms (WCICI & WOCICI).

4.1.2. SU-MIMO @8 BS antenna elements @10 ms SRS periodicity: 2SRS UE, 1SRSAS UE, 1SRSWOAS UE

Fig. 4.8 (2SRS UE), Fig. 4.9 (1SRSAS UE), and Fig. 4.10 (1SRWOAS UE), illustrate average downlink throughput per cell, SU-MIMO case with 8 BS antenna elements, FTP traffic profile, 10 ms sounding periodicity, and 3, 30 and 60 km/h UE moving speeds.

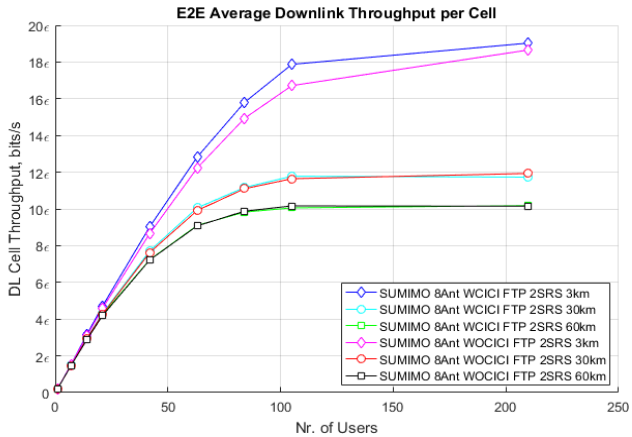

Figure 4.8: Average downlink throughput/cell @SU-MIMO_8 BS antenna elements @2SRS UE @10ms SRS periodicity @FTP

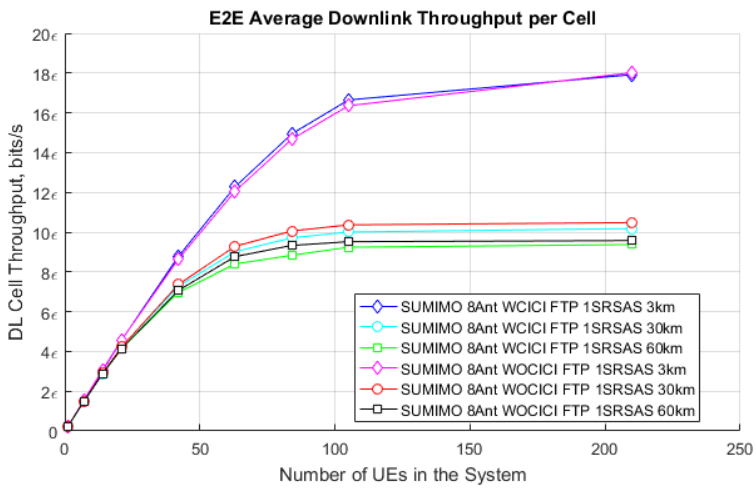

Figure 4.9: Average downlink throughput/cell @SU-MIMO_8 BS antenna elements @1SRSAS UE @10ms SRS periodicity @FTP

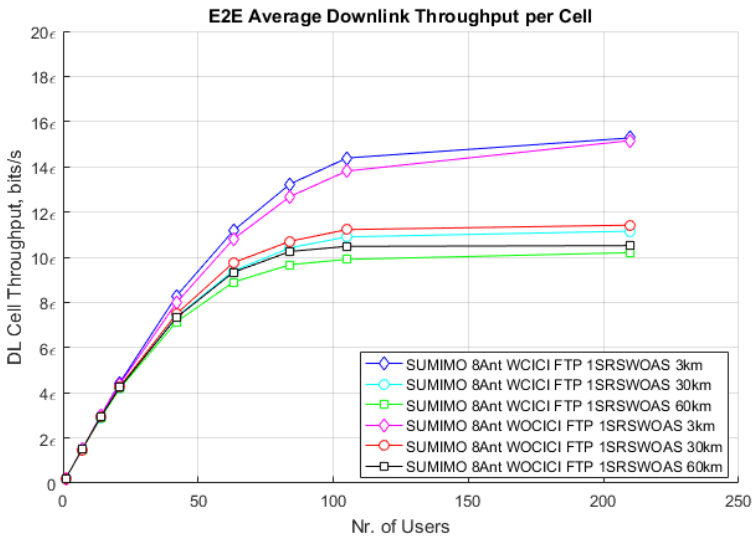

Figure 4.10: Average downlink throughput/cell @SU-MIMO_8 BS antenna elements @1SRSWOAS UE @10ms SRS periodicity @FTP

From Fig. 4.8, Fig. 4.9, and Fig. 4.10, the following observations can be made:

- **Fig. 4.8, Fig. 4.9, and Fig. 4.10:** In general, the average downlink throughput per cell decreases with increasing UE speeds for both algorithms (WCICI & WOCICI) and that is because of larger Doppler spreads.
- **Fig. 4.8:** Algorithm 2 (WCICI) outperforms algorithm 1 (WOCICI) in terms of average downlink throughput per cell for 3km/h UEs speed. However, for 30 and 60 km/h UE speeds, both algorithms (WCICI & WOCICI) offer almost the same performance.
- **Fig. 4.9:** Both algorithms (WCICI & WOCICI) offer almost the same performance in terms of average downlink throughput per cell for 3 km/h UE speed. However, for 30 and 60 km/h UE speeds, algorithm 1 (WOCICI) outperforms slightly algorithm 2 (WCICI).
- **Fig. 4.10:** Algorithm 2 (WCICI) outperforms algorithm 1 (WOCICI) in terms of average downlink throughput per cell for 3km/h UEs speed. However, for 30 and 60 km/h UE speeds, it is the opposite.

Fig. 4.11 (2SRS UE), Fig. 4.12 (1SRSAS UE), and Fig. 4.13 (1SRSWOAS UE), illustrate User throughput vs. Average served traffic per cell, SU-MIMO case with 8 BS antenna elements, FTP traffic profile, 10 ms sounding periodicity, and 3, 30 and 60 km/h UE moving speeds.

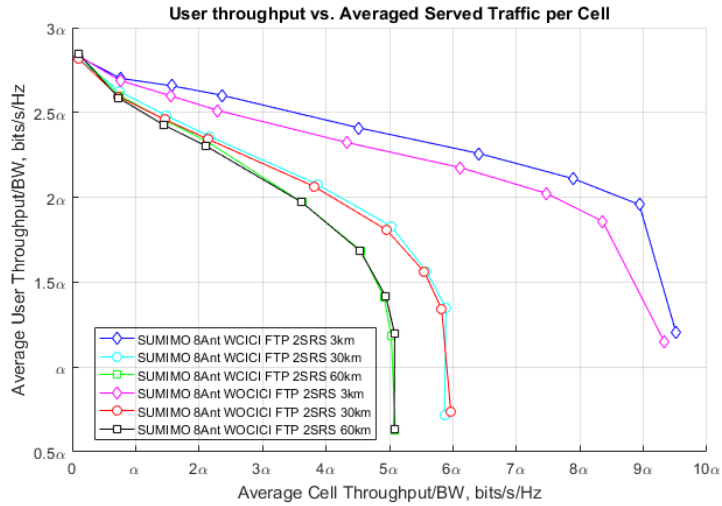

Figure 4.11: User throughput vs. Average served traffic per cell @SU-MIMO_8 BS antenna elements @2SRS UE @10ms SRS periodicity @FTP

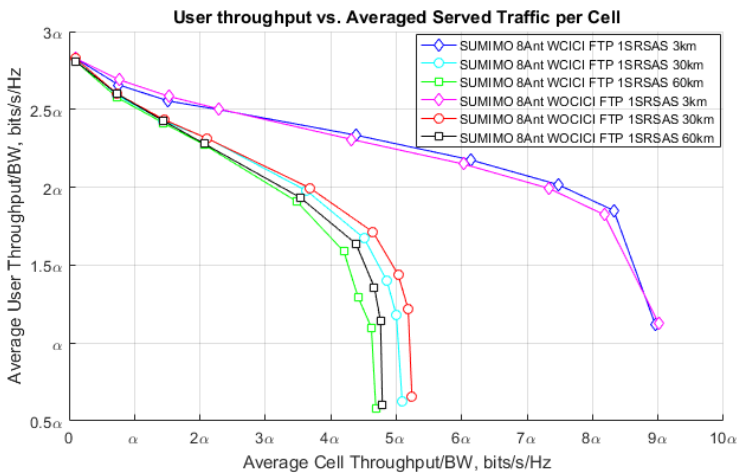

Figure 4.12: User throughput vs. Average served traffic per cell @SU-MIMO_8 BS antenna elements @1SRSAS UE @10ms SRS periodicity @FTP

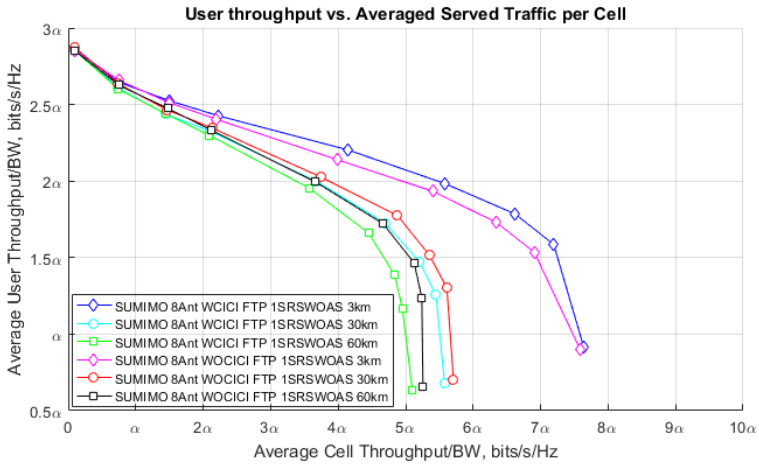

Figure 4.13: User throughput vs. Average served traffic per cell @SU-MIMO_8 BS antenna elements @1SRSWOAS UE @10ms SRS periodicity @FTP

Fig. 4.11, Fig. 4.12, and Fig. 4.13 can be interpreted in the following way:

- **Fig. 4.11, Fig. 4.12, and Fig. 4.13:** The number of UEs to be optimally handled decreases with increasing UE speed for a given user throughput-spectral efficiency threshold for both algorithms (WCICI & WOCICI).
- **Fig. 4.11:** For a user throughput-spectral efficiency threshold of 2α bits/sec/Hz as an example, the system can handle optimally 84 for 3 km/h UEs speed and approximately 42 UEs for 30 km/h and 60 km/h UE speeds with both algorithms (WCICI & WOCICI).
- **Fig. 4.12:** For a user throughput-spectral efficiency threshold of 2α bits/sec/Hz as an example, the system can handle optimally 84 UEs for 3 km/h UE speed and approximately 42 UEs for 30 and 60 km/h UE speeds with both algorithms (WCICI & WOCICI).
- **Fig. 4.13:** For a user throughput-spectral efficiency threshold of 2α bits/sec/Hz as an example, the system can handle optimally 63 UEs for 3 km/h UE speed and approximately 42 UEs for 30 and 60 km/h UE speeds with both algorithms (WCICI & WOCICI).

4.1.3. SU-MIMO @8 BS antenna elements @20 ms SRS periodicity: 2SRS UE, 1SRSAS UE, 1SRSWOAS UE

Fig. 4.14 (2SRS UE), Fig. 4.15 (1SRSAS UE), and Fig. 4.16 (1SRWOAS UE), illustrate average downlink throughput per cell, SU-MIMO case with 8 BS antenna elements, FTP traffic profile, 20 ms sounding periodicity, and 3, 30 and 60 km/h UE moving speeds.

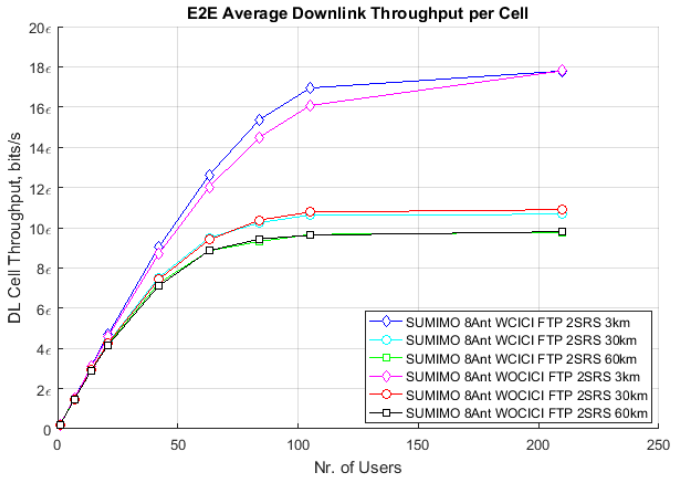

Figure 4.14: Average downlink throughput/cell @SU-MIMO_8 BS antenna elements @2SRS UE @20ms SRS periodicity @FTP

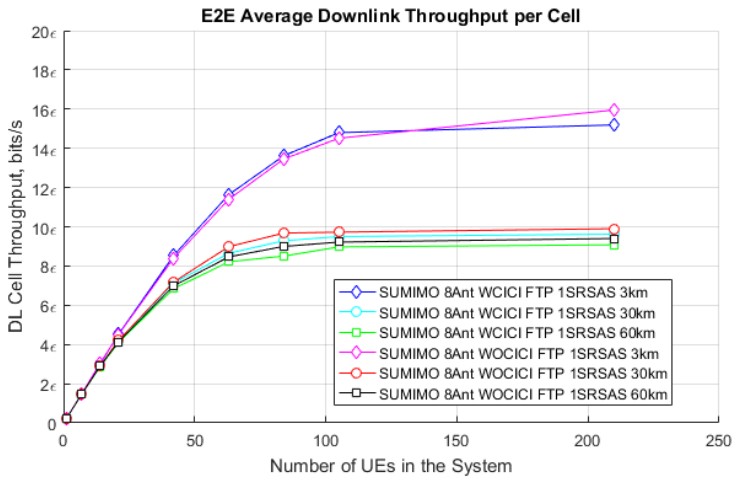

Figure 4.15: Average downlink throughput/cell @SU-MIMO_8 BS antenna elements @1SRSAS UE @20ms SRS periodicity @FTP

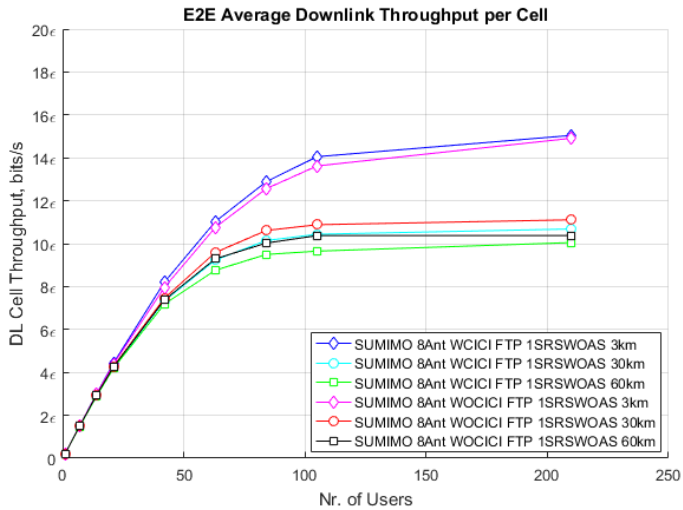

Figure 4.16: Average downlink throughput/cell @SU-MIMO_8 BS antenna elements @1SRSWOAS UE @20ms SRS periodicity @FTP

From Fig. 4.14, Fig. 4.15, and Fig. 4.16, the following observations can be made:

- **Fig. 4.14, Fig. 4.15, and Fig. 4.16:** In general, the average downlink throughput decreases with increasing UE speeds for both algorithms (WCICI & WOCICI) and that is because of larger Doppler spreads.
- **Fig. 4.14:** Algorithm 2 (WCICI) outperforms algorithm 1 (WOCICI) in terms of average downlink throughput per cell for 3km/h UEs speed. However, for 30 and 60 km/h UE speeds, both algorithms (WCICI & WOCICI) offer almost the same performance.
- **Fig. 4.15:** Both algorithms (WCICI & WOCICI) offer almost the same performance in terms of average downlink throughput per cell for 3 km/h UE speed up to approximately 140 UEs. Above 140 UEs, algorithm 1 (WOCICI) outperforms algorithm 2 (WCICI). However, for 30 and 60 km/h UE speeds, algorithm 1 (WOCICI) outperforms slightly algorithm 2 (WCICI).
- **Fig. 4.16:** Algorithm 2 (WCICI) outperforms algorithm 1 (WOCICI) in terms of average downlink throughput per cell for 3km/h UEs speed. However, for 30 and 60 km/h UE speeds, it is the opposite.

Fig. 4.17 (2SRS UE), Fig. 4.18 (1SRSAS UE), and Fig. 4.19 (1SRSWOAS UE), illustrate User throughput vs. Average served traffic per cell, SU-MIMO case with 8 BS antenna elements, FTP traffic profile, 20 ms sounding periodicity, and 3, 30 and 60 km/h UE moving speeds.

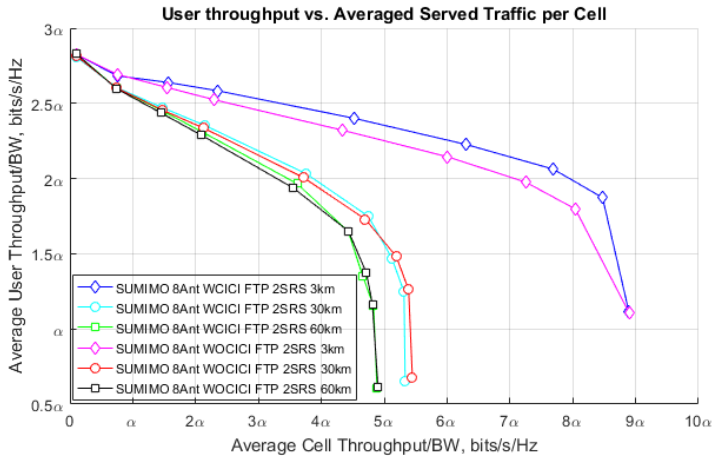

Figure 4.17: User throughput vs. Average served traffic per cell @SU-MIMO_8 BS antenna elements @2SRS UE @20ms SRS periodicity @FTP

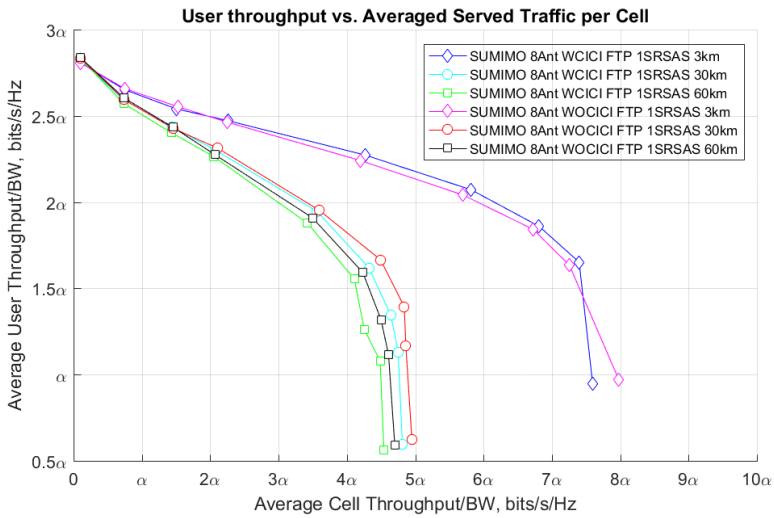

Figure 4.18: User throughput vs. Average served traffic per cell @SU-MIMO_8 BS antenna elements @1SRSAS UE @20ms SRS periodicity @FTP

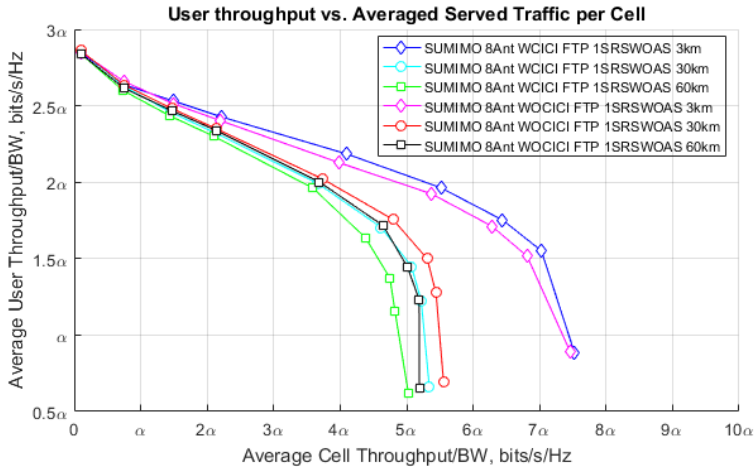

Figure 4.19: User throughput vs. Average served traffic per cell @SU-MIMO_8 BS antenna elements @1SRSWOAS UE @20ms SRS periodicity @FTP

Fig. 4.17, Fig. 4.18, and Fig. 4.19 can be interpreted in the following way:

- **Fig. 4.17, Fig. 4.18, and Fig. 4.19:** The number of UEs to be optimally handled decreases with increasing UE speed for a given user throughput-spectral efficiency threshold for both algorithms (WCICI & WOCICI).
- **Fig. 4.17:** For a user throughput-spectral efficiency threshold of 2α bits/sec/Hz as an example, the system can handle optimally 84 UEs for 3 km/h UEs speed and approximately 42 UEs for 30 km/h and 60 km/h UE speeds with both algorithms (WCICI & WOCICI).
- **Fig. 4.18:** For a user throughput-spectral efficiency threshold of 2α bits/sec/Hz as an example, the system can handle optimally 63 UEs for 3 km/h UE speed and approximately between 21 and 42 UEs for 30 and 60 km/h UE speeds with both algorithms (WCICI & WOCICI).
- **Fig. 4.19:** For a user throughput-spectral efficiency threshold of 2α bits/sec/Hz as an example, the system can handle optimally 63 UEs for 3 km/h UE speed and approximately 42 UEs for 30 and 60 km/h UE speeds with both algorithms (WCICI & WOCICI).

4.2. SU-MIMO (Full-Buffer traffic profile and 64 BS antenna elements)

The main simulation parameters for SU-MIMO with Full-Buffer traffic profile and 64 BS antenna elements (BSULA topology: 4x8x2**)** are given in Table 4.2.

Table 4.2: Simulation parameters for SU-MIMO with Full-Buffer traffic profile and 64 BS antennas elements (BSULA topology: 4x8x2)

System bandwidth	20MHz
Frame configuration	TDD (2 UL subframes per frame)
Number of DL layers	2
Number of BS antenna elements	64
Beamforming weights	With and without considering ICI
Propagation model	2D SCM Urban macro environment
7 sites x 3 sectors	21 cells, 3GPP case 1 (ISD 500m)
SRS (sounding) bandwidth	96 PRBs (Full-bandwidth)
SRS (sounding) periodicity (ms)	[5, 10, 20]
SRS UL antenna configuration	2SRS UE, 1SRSAS UE, 1SRSWOAS UE
UE speed (km/h)	[3, 30, 60]
UE traffic profile	Full-Buffer
Scheduling strategy	Round Robin
Seeds	10, 10.005 seconds/seed
Number users as iteration variable	[1,7,14,21,42,63,84,105,210]

4.2.1. SU-MIMO @64 BS antenna elements @5 ms SRS periodicity: 2SRS UE, 1SRSAS UE, 1SRSWOAS UE

Fig. 4.20 (2SRS UE), Fig. 4.21 (1SRSAS UE), and Fig. 4.22 (1SRWOAS UE), illustrate average downlink throughput per cell, SU-MIMO case with 64 BS antenna elements, Full-Buffer traffic profile, 5 ms sounding periodicity, and 3, 30 and 60 km/h UE moving speeds.

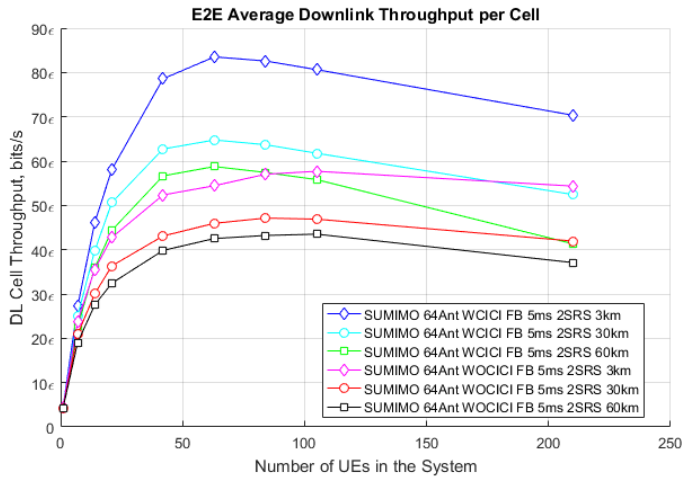

Figure 4.20: Average downlink throughput/cell @SU-MIMO_64 BS antenna elements @2SRS UE @5ms SRS periodicity @Full-Buffer

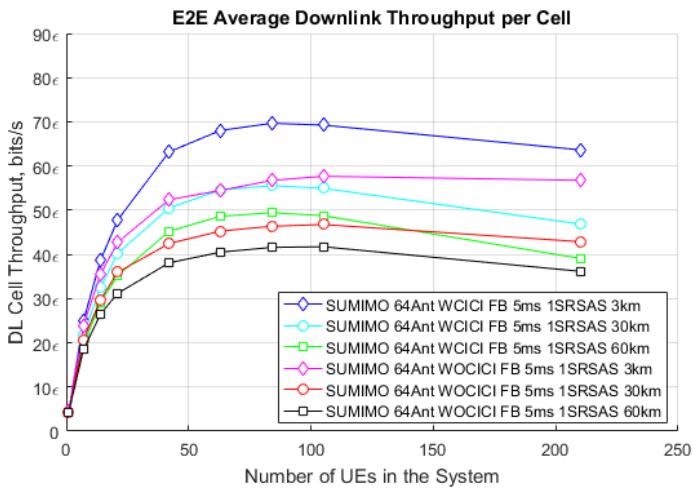

Figure 4.21: Average downlink throughput/cell @SU-MIMO_64 BS antenna elements @1SRSAS UE @5ms SRS periodicity @Full-Buffer

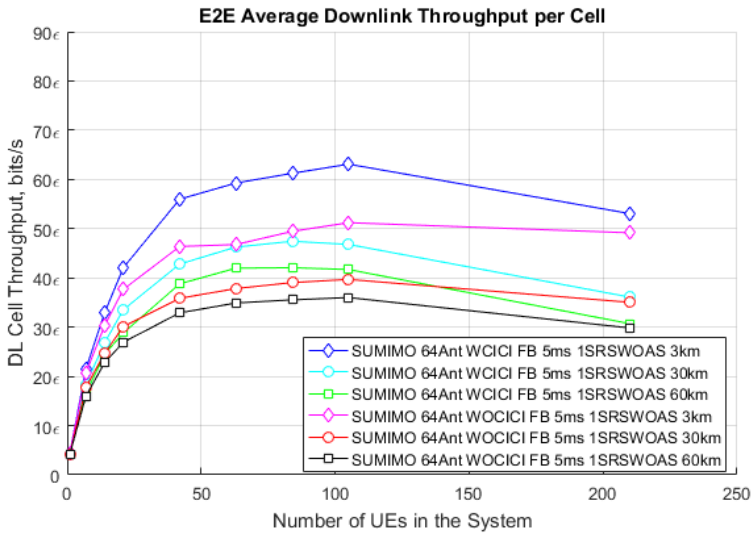

Figure 4.22: Average downlink throughput/cell @SU-MIMO_64 BS antenna elements @1SRSWOAS UE @5ms SRS periodicity @Full-Buffer

From Fig. 4.20, Fig. 2.21, and Fig. 2.22 the following observations can be made:

- **Fig. 4.20, Fig. 4.21, and Fig. 4.22:** In general, the average downlink throughput decreases with increasing UE speeds for both algorithms (WCICI & WOCICI) and that is because of larger Doppler spreads.
- **Fig. 4.20:** Algorithm 2 (WCICI) outperforms algorithm 1 (WOCICI) in terms of average downlink throughput per cell for 3, 30 and 60 km/h UE speed.
- **Fig. 4.21:** Algorithm 2 (WCICI) outperforms algorithm 1 (WOCICI) in terms of average downlink throughput per cell for 3, 30 and 60 km/h UE speed.
- **Fig. 4.22:** Algorithm 2 (WCICI) outperforms algorithm 1 (WOCICI) in terms of average downlink throughput per cell for 3, 30 and 60 km/h UE speed.

Fig. 4.23 (2SRS UE), Fig. 4.24 (1SRSAS UE), and Fig. 4.25 (1SRSWOAS UE), illustrate User throughput vs. Average served traffic per cell, SU-MIMO case with 64 BS antenna elements, Full-Buffer traffic profile, 5 ms sounding periodicity, and 3, 30 and 60 km/h UE moving speeds.

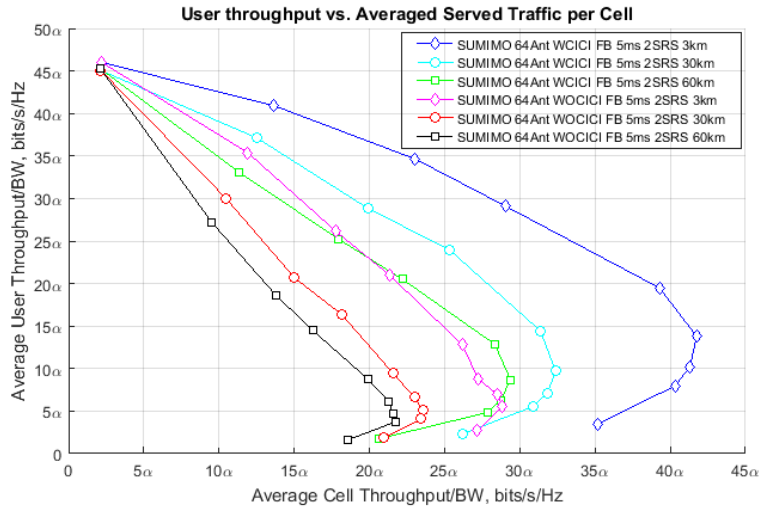

Figure 4.23: User throughput vs. Average served traffic per cell @SU-MIMO_64 BS antenna elements @2SRS UE @5ms SRS periodicity @Full-Buffer

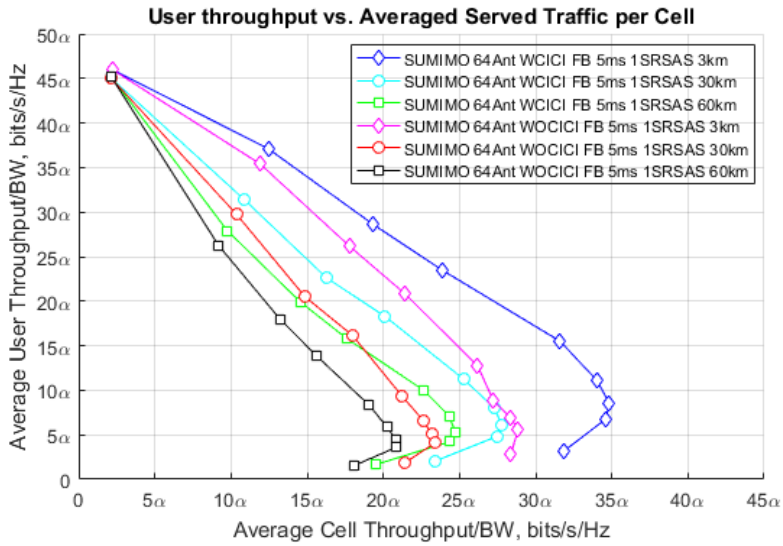

Figure 4.24: User throughput vs. Average served traffic per cell @SU-MIMO_64 BS antenna elements @1SRSAS UE @5ms SRS periodicity @Full-Buffer

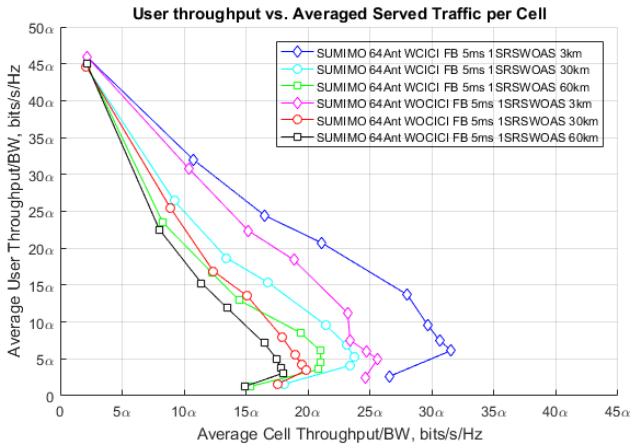

Figure 4.25: User throughput vs. Average served traffic per cell @SU-MIMO_64 BS antenna elements @1SRSWOAS UE @5ms SRS periodicity @Full-Buffer

Fig. 4.23, Fig. 4.24, and Fig. 4.25 can be interpreted in the following way:

- **Fig. 4.23, Fig. 4.24, and Fig. 4.25:** The number of UEs to be optimally handled decreases with increasing UE speed for a given user throughput-spectral efficiency threshold for both algorithms (WCICI & WOCICI).
- **Fig. 4.23:** For a user throughput-spectral efficiency threshold of 10α bits/sec/Hz as an example, the system can handle approximately 63 UEs with algorithm 1 (WOCICI) and 84 UEs with algorithm 2 (WCICI) for 3 km/h UE speed, and 42 UEs with algorithm 1 (WOCICI) and 63 UEs with algorithm 2 (WCICI) for 30 km/h UE speed, and approximately 42 UEs with both algorithms (WCICI & WOCICI) for 60 km/h UE speed.
- **Fig. 4.24:** For a user throughput-spectral efficiency threshold of 10α bits/sec/Hz as an example, the system can handle optimally 63 UEs for 3 km/h UE speed, and 42 UEs for 30 and 60 km/h UE speeds with both algorithms (WCICI & WOCICI).
- **Fig. 4.25:** For a user throughput-spectral efficiency threshold of 10α bits/sec/Hz as an example, the system can handle optimally 42 UEs with algorithm 1 (WOCICI) and 63 UEs with algorithm 2 (WCICI) for 3 km/h UE speed, and 21 UEs with algorithm 1 (WOCICI) and 42 UEs with algorithm 2 (WCICI) for 30 km/h UE speed, and 21

UEs with both algorithms (WCICI & WOCICI) for 60 km/h UE speed.

4.2.2. SU-MIMO @64 BS antenna elements @10 ms SRS periodicity: 2SRS UE, 1SRSAS UE, 1SRSWOAS UE

Fig. 4.26 (2SRS UE), Fig. 4.27 (1SRSAS UE), and Fig. 4.28 (1SRWOAS UE), illustrate average downlink throughput per cell, SU-MIMO case with 64 BS antenna elements, Full-Buffer traffic profile, 10 ms sounding periodicity, and 3, 30 and 60 km/h UE moving speeds.

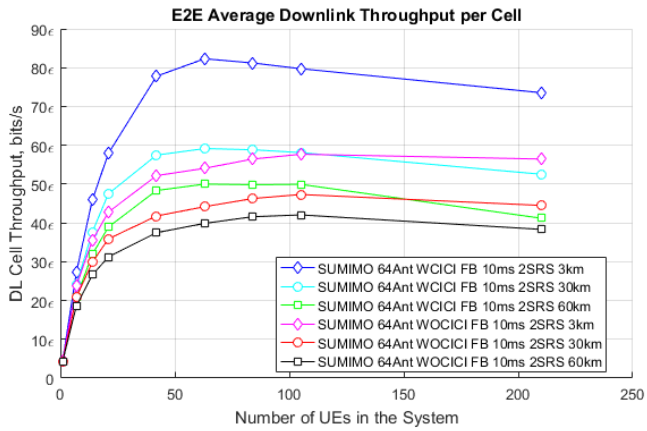

Figure 4.26: Average downlink throughput/cell @SU-MIMO_64 BS antenna elements @2SRS UE @10 ms SRS periodicity @Full-Buffer

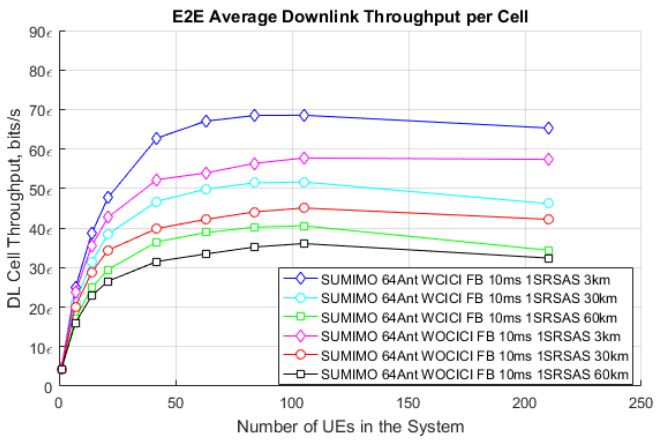

Figure 4.27: Average downlink throughput/cell @SU-MIMO_64 BS antenna elements @1SRSAS UE @10 ms SRS periodicity @Full-Buffer

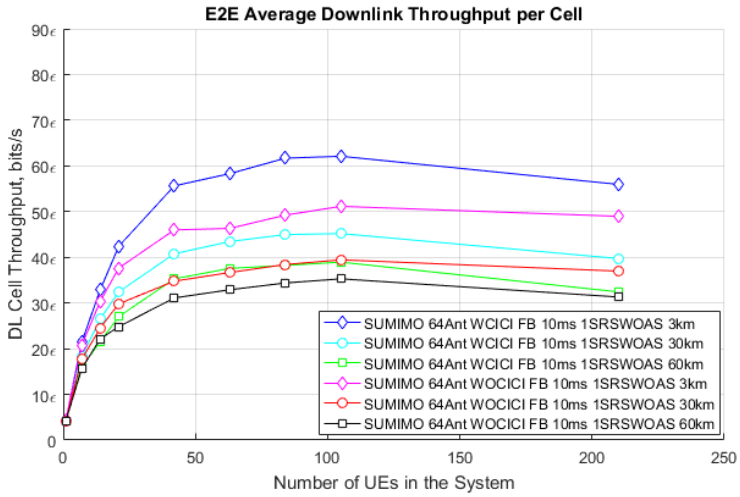

Figure 4.28: Average downlink throughput/cell @SU-MIMO_64 BS antenna elements @1SRSWOAS UE @10 ms SRS periodicity @Full-Buffer

From Fig. 4.26, Fig. 4.27, and Fig. 4.28, the following observations can be made:

- **Fig. 4.26, Fig. 4.27, and Fig. 4.28:** In general, the average downlink throughput decreases with increasing UE speeds for both algorithms (WCICI & WOCICI) and that is because of larger Doppler spreads.
- **Fig. 4.26:** Algorithm 2 (WCICI) outperforms algorithm 1 (WOCICI) in terms of average downlink throughput per cell for 3, 30 and 60 km/h UE speed.
- **Fig. 4.27:** Algorithm 2 (WCICI) outperforms algorithm 1 (WOCICI) in terms of average downlink throughput per cell for 3, 30 and 60 km/h UE speed.
- **Fig. 4.28:** Algorithm 2 (WCICI) outperforms algorithm 1 (WOCICI) in terms of average downlink throughput per cell for 3, 30 and 60 km/h UE speed.

Fig. 4.29 (2SRS UE), Fig. 4.30 (1SRSAS UE), and Fig. 4.31 (1SRSWOAS UE), illustrate User throughput vs. Average served traffic per cell, SU-MIMO case with 64 BS antenna elements, Full-Buffer traffic profile, 10 ms sounding periodicity, and 3, 30 and 60 km/h UE moving speeds.

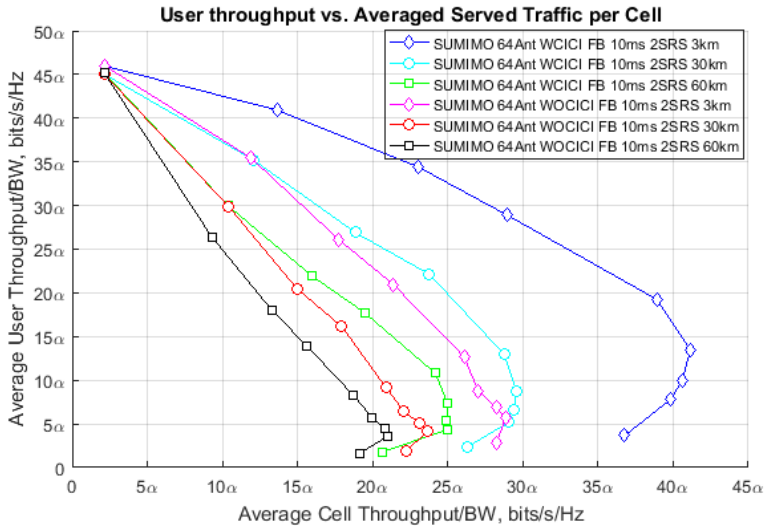

Figure 4.29: User throughput vs. Average served traffic per cell @SU-MIMO_64 BS antenna elements @2SRS UE @10ms SRS periodicity @Full-Buffer

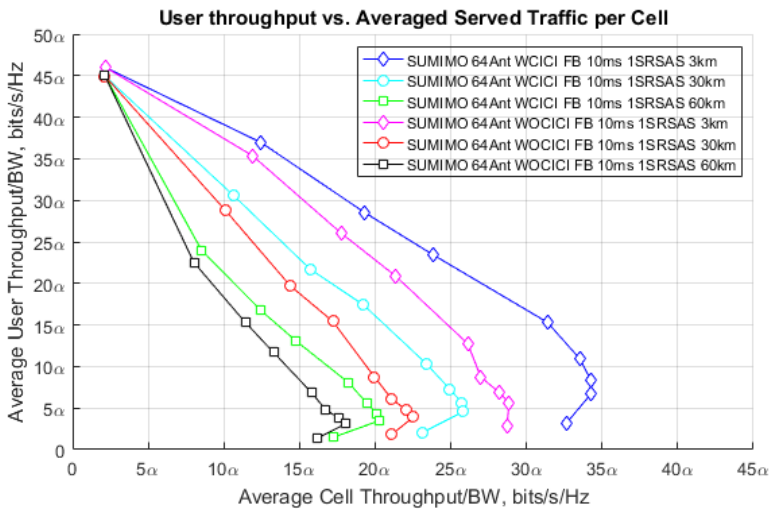

Figure 4.30: User throughput vs. Average served traffic per cell @SU-MIMO_64 BS antenna elements @1SRSAS UE @10ms SRS periodicity @Full-Buffer

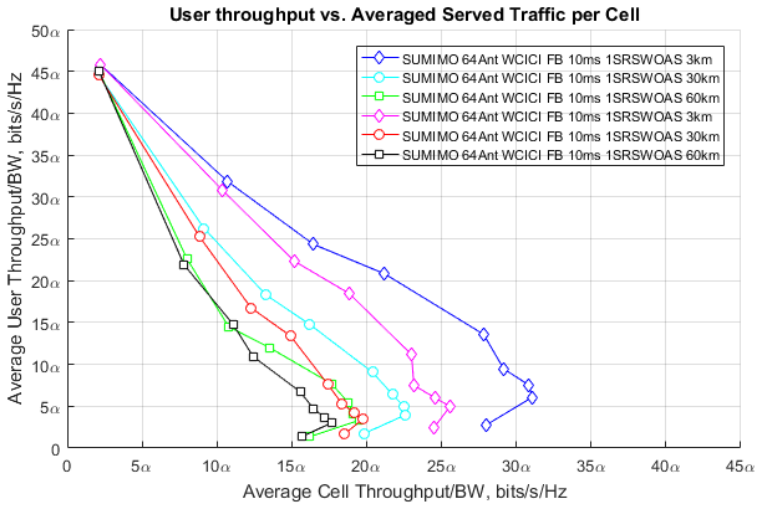

Figure 4.31: User throughput vs. Average served traffic per cell @SU-MIMO_64 BS antenna elements @1SRSWOAS UE @10ms SRS periodicity @Full-Buffer

Fig. 4.29, Fig. 4.30, and Fig. 4.31 can be interpreted in the following way:

- **Fig. 4.29, Fig. 4.20, and Fig. 4.31:** The number of UEs to be optimally handled decreases with increasing UE speed for a given user throughput-spectral efficiency threshold for both algorithms (WCICI & WOCICI).
- **Fig. 4.29:** For a user throughput-spectral efficiency threshold of 10α bits/sec/Hz as an example, the system can handle approximately 63 UEs with algorithm 1 (WOCICI) and 84 UEs with algorithm 2 (WCICI) for 3 km/h UE speed, and 42 UEs with algorithm 1 (WOCICI) and 63 UEs with algorithm 2 (WCICI) for 30 km/h, and 42 UEs with both algorithms (WCICI & WOCICI) for 60 km/h UE speed.
- **Fig. 4.30:** For a user throughput-spectral efficiency threshold of 10α bits/sec/Hz as an example, the system can handle optimally 63 UEs for 3 km/h UE speed, 42 UEs for 30 km/h UE speed, and 21 UEs for 60 km/h UE speed with both algorithms (WCICI & WOCICI).
- **Fig. 4.31:** For a user throughput-spectral efficiency threshold of 10α bits/sec/Hz as an example, the system can handle optimally

42 UEs with algorithm 1 (WOCICI) and 63 UEs with algorithm 2 (WCICI) for 3 km/h UE speed, and 21 UEs with algorithm 1 (WOCICI) and 42 UEs with algorithm 2 (WCICI) for 30 km/h UE speed, and 21 UEs with both algorithms (WCICI & WOCICI) for 60 km/h UE speed.

4.2.3. SU-MIMO @64 BS antenna elements @20 ms SRS periodicity: 2SRS UE, 1SRSAS UE, 1SRSWOAS UE

Fig. 4.32 (2SRS UE), Fig. 4.33 (1SRSAS UE), and Fig. 4.34 (1SRWOAS UE), illustrate average downlink throughput per cell, SU-MIMO case with 64 BS antenna elements, Full-Buffer traffic profile, 20 ms sounding periodicity, and 3, 30 and 60 km/h UE moving speeds.

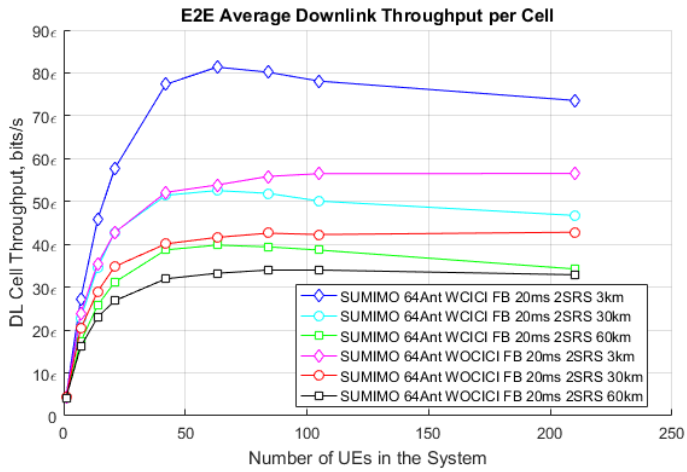

Figure 4.32: Average downlink throughput/Cell @SU-MIMO_64 BS antenna elements @2SRS UE @20 ms SRS periodicity @Full-Buffer

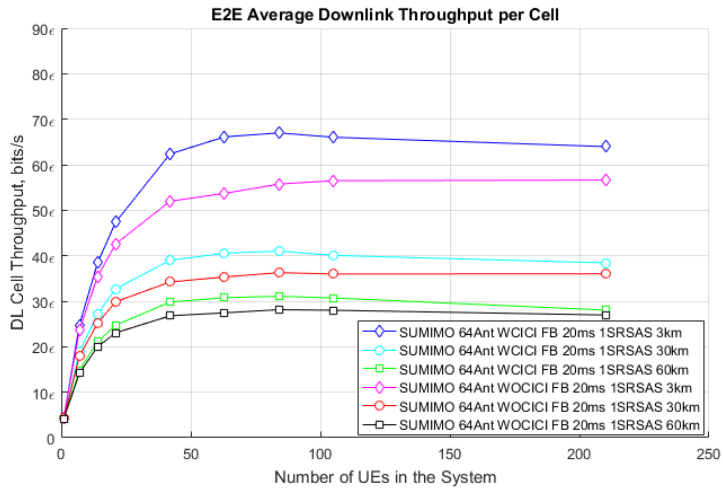

Figure 4.33: Average downlink throughput/cell @SU-MIMO_64 BS antenna elements @1SRSAS UE @20 ms SRS periodicity @Full-Buffer

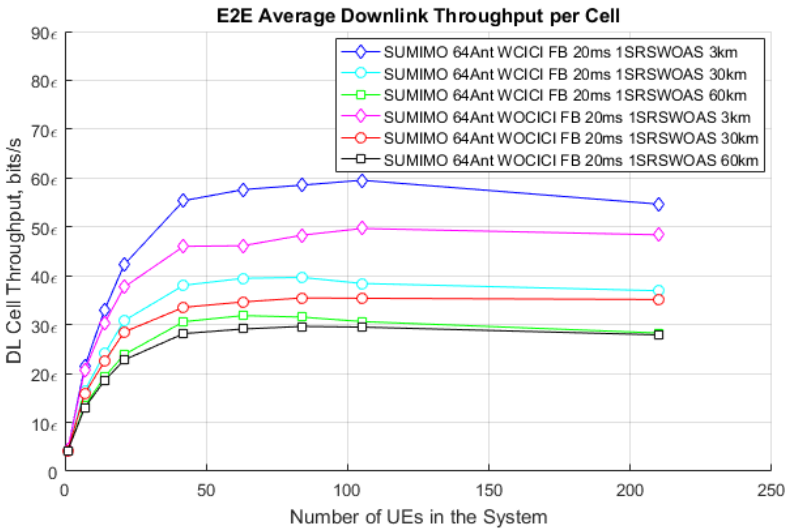

Figure 4.34: Average downlink throughput/cell @SU-MIMO_64 BS antenna elements @1SRSWOAS UE @20 ms SRS periodicity @Full-Buffer

From Fig. 4.32, Fig. 4.33, and Fig. 4.34, the following observations can be made:

- **Fig. 4.32, Fig. 4.33, and Fig. 4.34:** In general, the average downlink throughput decreases with increasing UE speeds for both algorithms (WCICI & WOCICI) and that is because of larger Doppler spreads.
- **Fig. 4.32:** Algorithm 2 (WCICI) outperforms algorithm 1 (WOCICI) in terms of average downlink throughput per cell for 3, 30 and 60 km/h UE speed.
- **Fig. 4.33:** Algorithm 2 (WCICI) outperforms algorithm 1 (WOCICI) in terms of average downlink throughput per cell for 3, 30 and 60 km/h UE speed.
- **Fig. 4.34:** Algorithm 2 (WCICI) outperforms algorithm 1 (WOCICI) in terms of average downlink throughput per cell for 3, 30 and 60 km/h UE speed.

Fig. 4.35 (2SRS UE), Fig. 4.36 (1SRSAS UE), and Fig. 4.37 (1SRSWOAS UE), illustrate User throughput vs. Average served traffic per cell, SU-MIMO case with 64 BS antenna elements, Full-Buffer traffic profile, 20 ms sounding periodicity, and 3, 30 and 60 km/h UE moving speeds.

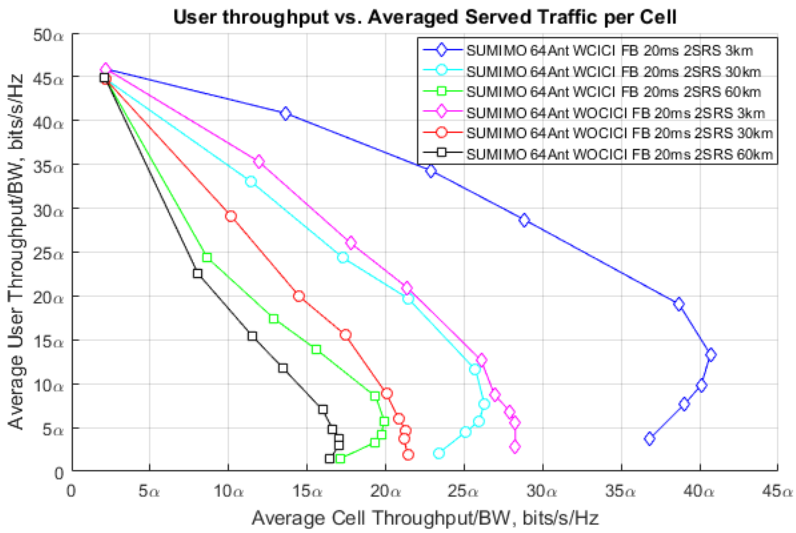

Figure 4.35: User throughput vs. Average served traffic per cell @SU-MIMO_64 BS antenna elements @2SRS UE @20ms SRS periodicity @Full-Buffer

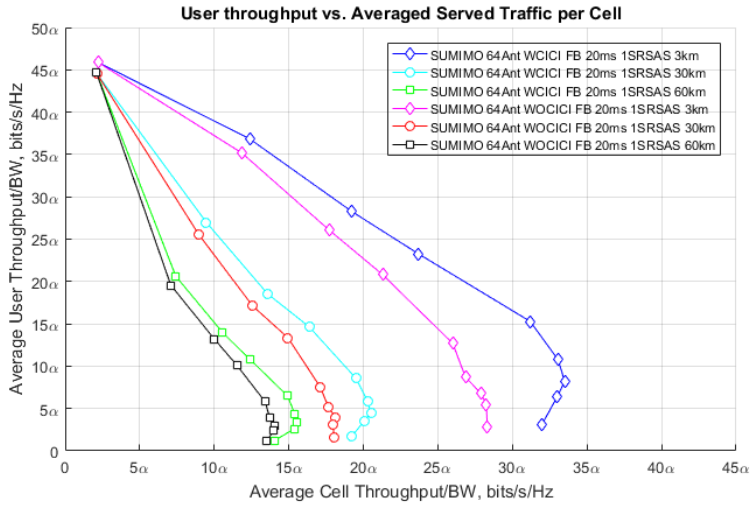

Figure 4.36: User throughput vs. Average served traffic per cell @SU-MIMO_64 BS antenna elements @1SRSAS UE @20ms SRS periodicity @Full-Buffer

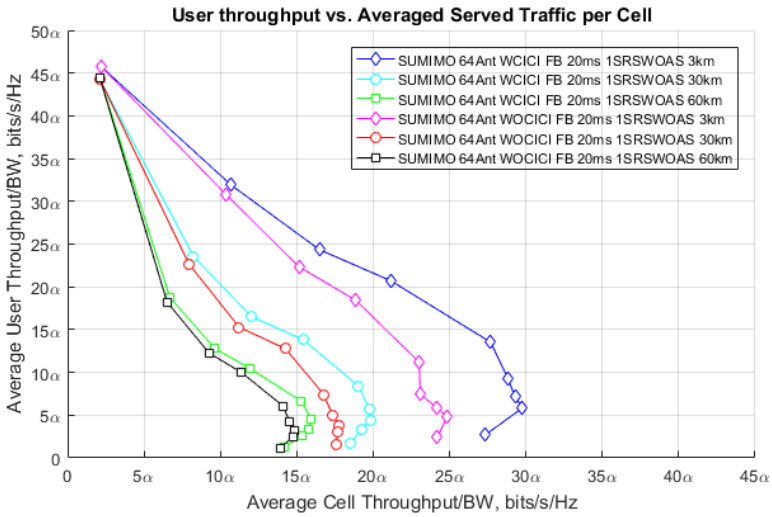

Figure 4.37: User throughput vs. Average served traffic per cell @SU-MIMO_64 BS antenna elements @1SRSWOAS UE @20ms SRS periodicity @Full-Buffer

Fig. 4.35, Fig. 4.36, and Fig. 4.37 can be interpreted in the following way:

- **Fig. 4.35, Fig. 4.36, and Fig. 4.37:** The number of UEs to be optimally handled decreases with increasing UE speed for a given user throughput-spectral efficiency threshold for both algorithms (WCICI & WOCICI).
- **Fig. 4.35:** For a user throughput-spectral efficiency threshold of 10α bits/sec/Hz as an example, the system can handle optimally 63 UEs with algorithm 1 (WOCICI) and 84 UEs with algorithm 2 (WCICI) for 3 km/h UE speed, and 42 UEs with Algorithm 1 (WOCICI) and approximately 63 UEs with algorithm 2 (WCICI) for 30 km/h UE speed, and between 21 and 42 UEs with both algorithms (WCICI & WOCICI) for 60 km/h UE speed.
- **Fig. 4.36:** For a user throughput-spectral efficiency threshold of 10α bits/sec/Hz as an example, the system can handle approximately 63 UEs with both algorithms (WCICI & WOCICI) for 3 km/h UE speed, and 42 UEs for 30km/h UE speed, and 21 UEs for 60 km/h UE speed with both algorithms (WCICI & WOCICI).
- **Fig. 4.37:** For a user throughput-spectral efficiency threshold of 10α bits/sec/Hz as an example, the system can handle optimally 42 UEs with Algorithm 1 (WOCICI) and 63 UEs with Algorithm 2 (WCICI) for 3 km/h UE speed, and between 21 and 42 UEs with both algorithms (WCICI & WOCICI) for 30 and 60 km/h UE speeds.

4.3. MU-MIMO (Full-Buffer traffic profile and 64 BS antennas elements)

The main simulation parameters for MU-MIMO with Full-Buffer traffic profile and 64 BS antennas elements (BSULA topology: 4x8x2**)** are given in Table 4.3.

Table 4.3: Simulation parameters for MU-MIMO with Full-Buffer traffic profile and 64 BS antennas elements (BSULA topology: 4x8x2)

System bandwidth	20MHz
Frame configuration	TDD (2 UL subframes per frame)
Number of DL layers	2
Number of BS antenna elements	64
Beamforming weights	With and without considering ICI
Propagation model	2D SCM Urban macro environment
7 sites x 3 sectors	21 cells, 3GPP case 1 (ISD 500m)
SRS (sounding) bandwidth	96 PRBs (Full-bandwidth)
SRS (sounding) periodicity (ms)	[5, 10, 20]
SRS UL antenna configuration	2SRS UE, 1SRSAS UE, 1SRSWOAS UE
UE speed (km/h)	[3, 30, 60]
UE traffic profile	Full-Buffer
Scheduling strategy	Round Robin
Seeds	10, 10.005 seconds/seed
Number users as iteration variable	[1,7,14,21,42,63,84,105,210]
Pairing limit	8 Layers (4 UEs with 2 layer each)
Orthogonality factor	[0.1, 0.25, 1]

4.3.1. MU-MIMO @64 BS antenna elements @2 SRS UE, UE speed: 3 km/h, Sounding periodicity: 5 ms

Fig. 4.38 (2SRS UE) illustrates average downlink throughput per cell, MU-MIMO case with 64 BS antenna elements, Full-Buffer traffic profile, 5 ms sounding periodicity, and 3 km/h UE moving speeds.

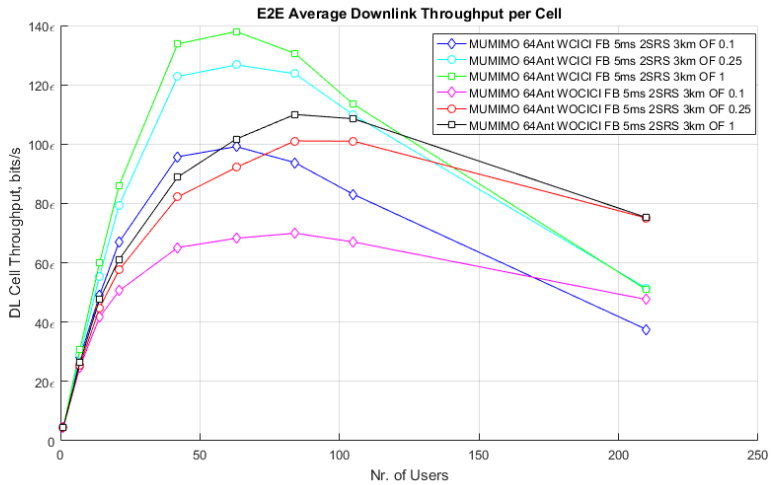

Figure 4.38: Average downlink throughput/cell @MU-MIMO @3 km/h @2SRS UE @5ms SRS periodicity @Full-Buffer

From Fig. 4.38, the following observations can be made:

- Algorithm 2 (WCICI) outperforms algorithm 1 (WOCICI) in terms of average downlink throughput per cell for orthogonality factor (OF) value of 1 and 3 km/h UEs speed up to approximately 120 users. For orthogonality factor (OF) value of 0.25 and 3 km/h UEs speed, algorithm 2 (WCICI) outperforms algorithm 1 (WOCICI) in terms of average downlink throughput per cell up to approximately 140 users. For orthogonality factor (OF) value of 0.1 and 3 km/h UEs speed, algorithm 2 (WCICI) outperforms algorithm 1(WOCICI) in terms of average downlink throughput per cell up to approximately 170 users.
- In general, a higher value of orthogonality factor (OF) implies a higher average downlink throughput per cell.

Fig. 4.39 (2SRS UE) illustrates User throughput vs. Average served traffic per cell, MU-MIMO case with 64 BS antenna elements, Full-Buffer traffic profile, 5 ms sounding periodicity, and 3 km/h UE moving speeds.

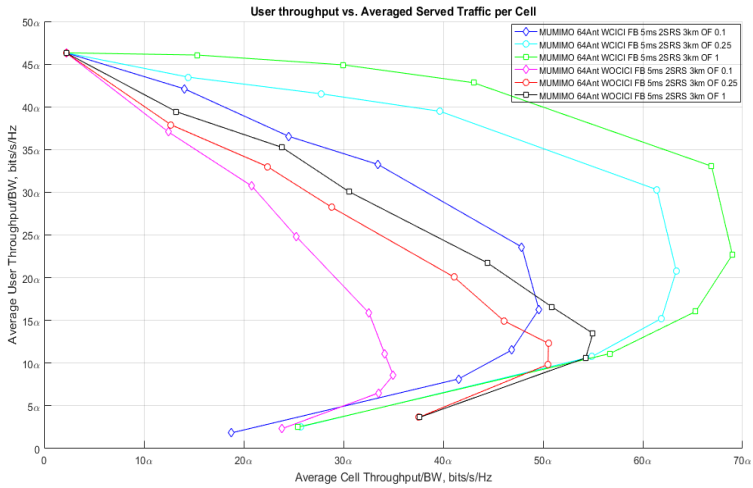

Figure 4.39: User throughput vs. Average served traffic per cell @MU-MIMO @3 km/h @2SRS UE @5ms SRS periodicity @Full-Buffer

Fig. 4.39 can be interpreted in the following way:

- In MU-MIMO with 3 km/h UE speed, for a user throughput-spectral efficiency threshold of 10α bits/sec/Hz as an example, the system can handle optimally 105 UEs with both algorithms (WCICI & WOCICI) for orthogonality factor value (OF) of 1.
- The number of UEs to be optimally handled in the system (MU-MIMO) decreases with increasing UE speed (compare Fig. 4.33 and Fig. 4.35).
- When the curves start bending, we can consider this point as an optimal performance of the system with the corresponding number of users.

4.3.2. MU-MIMO @64 BS antenna elements @2 SRS UE, UE speed: 30 km/h, Sounding periodicity: 5 ms

Fig. 4.40 (2SRS UE) illustrates average downlink throughput per cell, MU-MIMO case with 64 BS antenna elements, Full-Buffer traffic profile, 5 ms sounding periodicity, and 30 km/h UE moving speeds.

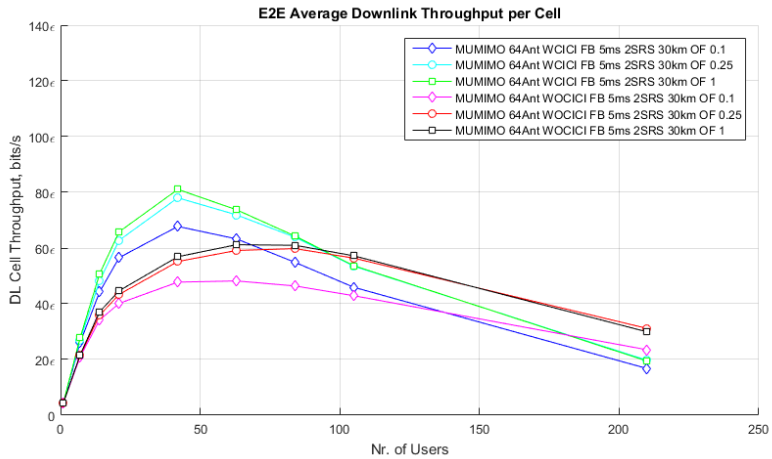

Figure 4.40: Average downlink throughput/cell @MU-MIMO @30 km/h @2SRS UE @5ms SRS periodicity @Full-Buffer

From Fig. 4.40, the following observations can be made:

- Algorithm 2 (WCICI) outperforms algorithm 1(WOCICI) in terms of average downlink throughput per cell for orthogonality factor (OF) values of 0.25 and 1 and 30 km/h UEs speed up to approximately 90 users. For orthogonality factor (OF) value of 0.1 and 30 km/h UEs speed, algorithm 2 (WCICI) outperforms algorithm 1 (WOCICI) in terms of average downlink throughput per cell up to approximately 140 users.
- In contrast the 3 km/h case, a higher value of orthogonality factor (OF) does not always imply a higher average downlink throughput per cell for both algorithms for 30 km/h UEs speed.

Fig. 4.41 (2 SRS UE) illustrates User throughput vs. Average served traffic per cell, MU-MIMO case with 64 BS antenna elements, Full-Buffer traffic profile, 5 ms sounding periodicity, and 30 km/h UE moving speeds.

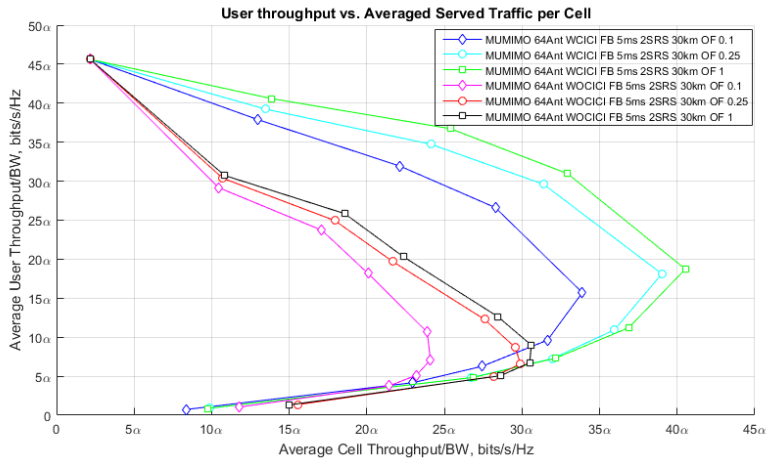

Figure 4.41: User throughput vs. Average served traffic per cell @MU-MIMO @30 km/h @2SRS UE @5ms SRS periodicity @Full-Buffer

Fig. 4.41 can be interpreted in the following way:

- In MU-MIMO with 30 km/h UE speed, for a user throughput-spectral efficiency threshold of 10α bits/sec/Hz as an example, the system can handle optimally 63 UEs with both algorithms (WCICI & WOCICI) for orthogonality factor value (OF) of 1.
- The number of UEs to be optimally handled in the system (MU-MIMO) decreases with increasing UE speed (compare Fig. 4.33 and Fig. 4.35).
- When the curves start bending, we can consider this point as an optimal performance of the system with the corresponding number of users.

4.4. Comparative analysis

In this section, the overall performance of both algorithms is summarized based on maximum cell throughput for the following cases: SU-MIMO (8 BS antenna elements and FTP traffic profile) in Section 4.4.1, SU-MIMO (64 BS antenna elements and Full-Buffer) in Section 4.4.2, and SU-MIMO vs. MU-MIMO (64 BS antenna elements and Full-Buffer traffic profile) in Section 4.4.3.

4.4.1. SU-MIMO (8 BS antenna elements and FTP traffic profile)

Table 4.4 summarizes Fig. 4.2, Fig. 4.3, and Fig. 4.4.

Table 4.4: Summary (Fig. 4.2, Fig. 4.3, and Fig. 4.4)

SU-MIMO @8 BS antenna elements @5 ms SRS periodicity @FTP		**Max_Thpt (bps) @3km/h @105users**	**Max_Thpt (bps) @30km/h @105users**	**Max_Thpt (bps) @60km/h @105users**
2SRS UE	WOCICI	~16.5ε	~13.5ε	~10.5ε
	WCICI	~18ε	~13.5ε	~10.5ε
1SRSAS UE	WOCICI	~16.5ε	~11ε	~10ε
	WCICI	~17ε	~11ε	~10ε
1SRSWOAS UE	WOCICI	~14ε	~11.5ε	~10.5ε
	WCICI	~14.5ε	~12ε	~10ε

Table 4.5 summarizes Fig. 4.8, Fig. 4.9, and Fig. 4.10.

Table 4.5: Summary (Fig. 4.8, Fig. 4.9, and Fig. 4.10)

SU-MIMO @8 BS antenna elements @10 ms SRS periodicity @FTP		**Max_Thpt (bps) @3km/h @105users**	**Max_Thpt (bps) @30km/h @105users**	**Max_Thpt (bps) @60km/h @105users**
2SRS UE	WOCICI	~16.5ε	~12ε	~10ε
	WCICI	~18ε	~12ε	~10ε
1SRSAS UE	WOCICI	~16ε	~10ε	~9.5ε
	WCICI	~16ε	~10ε	~9.5ε
1SRSWOAS UE	WOCICI	~14ε	~11ε	~10.5ε
	WCICI	~14.5ε	~11ε	~10ε

Table 4.6 summarizes Fig. 4.14, Fig. 4.15, and Fig. 4.16.

Table 4.6: Summary (Fig. 4.14, Fig. 4.15, and Fig. 4.16)

SU-MIMO @8 BS antenna elements @20 ms SRS periodicity @FTP		**Max_Thpt (bps) @3km/h @105users**	**Max_Thpt (bps) @30km/h @42users**	**Max_Thpt (bps) @60km/h @42users**
2SRS UE	WOCICI	~16ε	~10.5ε	~10.5ε
	WCICI	~17ε	~10.5ε	~9.5ε
1SRSAS UE	WOCICI	~15ε	~10ε	~9.5ε
	WCICI	~15ε	~10ε	~9.5ε
1SRSWOAS UE	WOCICI	~13.5ε	~11ε	~10.5ε
	WCICI	~14ε	~10.5ε	~9.5ε

From Table 4.4, Table 4.5, and Table 4.6, the following observations can be made:

- 2 SRS UE offers the best performance in terms of maximum cell throughput with both algorithms (WCICI & WOCICI) for 5, 10 and 20 ms SRS periodicities and all UE speeds.
- 1 SRSAS UE offers the medium performance in terms of maximum cell throughput with both algorithms (WCICI & WOCICI) for 5, 10 and 20 ms SRS periodicities and pedestrian users (3 km/h UE speed), but it is not the case for medium (30 km/h) and high (60 km/h) UE speeds where 1 SRSWOAS performs better that 1 SRSAS.
- For pedestrian users (3 km/h UE speed), the effect of SRS periodicity is negligible. However, for medium (30 km/h) and high mobility users (60 km/h), the effect of SRS periodicity is somewhat noticeable.
- There is degradation of maximum cell throughput with increasing SRS periodicity and UE speed.

4.4.2. SU-MIMO (64 BS antenna elements and Full-Buffer traffic profile)

Table 4.7 summarizes Fig. 4.20, Fig. 4.21, and Fig. 4.22.

Table 4.7: Summary (Fig. 4.20, Fig. 4.21, and Fig. 4.22)

SU-MIMO @64 BS antenna elements @5 ms SRS periodicity @Full-Buffer		**Max_Thpt (bps) @3km/h @63users**	**Max_Thpt (bps) @30km/h @63users**	**Max_Thpt (bps) @60km/h @63users**
2SRS UE	WOCICI	~54ε	~45ε	~41ε
	WCICI	~84ε	~65ε	~59ε
1SRSAS UE	WOCICI	~54ε	~45ε	~40ε
	WCICI	~78ε	~54ε	~48ε
1SRSWOAS UE	WOCICI	~47ε	~38ε	~35ε
	WCICI	~60ε	~47ε	~41ε

Table 4.8 summarizes Fig. 4.26, Fig. 4.27, and Fig. 4.28.

Table 4.8: Summary (Fig. 4.26, Fig. 4.27, and Fig. 4.28)

SU-MIMO @64 BS antenna elements @10 ms SRS periodicity @Full-Buffer		**Max_Thpt (bps) @3km/h @63users**	**Max_Thpt (bps) @30km/h @63users**	**Max_Thpt (bps) @60km/h @63users**
2SRS UE	WOCICI	~54ε	~44ε	~40ε
	WCICI	~82ε	~60ε	~50ε
1SRSAS UE	WOCICI	~54ε	~42ε	~33ε
	WCICI	~68ε	~50ε	~39ε
1SRSWOAS UE	WOCICI	~46ε	~36ε	~32ε
	WCICI	~60ε	~44ε	~36ε

Table 4.9 summarizes Fig. 4.32, Fig. 4.33, and Fig. 4.34.

Table 4.9: Summary (Fig. 4.32, Fig. 4.33, and Fig. 4.34)

SU-MIMO @8 BS antenna elements @20 ms SRS periodicity @Full-Buffer		**Max_Thpt (bps) @3km/h @105users**	**Max_Thpt (bps) @30km/h @105users**	**Max_Thpt (bps) @60km/h @105users**
2SRS UE	WOCICI	~54ε	~42ε	~34ε
	WCICI	~80ε	~52ε	~40ε
1SRSAS UE	WOCICI	~54ε	~35ε	~28ε
	WCICI	~66ε	~40ε	~30ε
1SRSWOAS UE	WOCICI	~46ε	~34ε	~29ε
	WCICI	~58ε	~40ε	~31ε

From Table 4.7, Table 4.8 and Table 4.9, the following observations can be made:

- 2 SRS UE offers the best performance in terms of maximum cell throughput with both algorithms (WCICI & WOCICI) for 5, 10 and 20 ms SRS periodicities and all UE speeds.
- 1 SRSAS UE offers the medium performance in terms of maximum cell throughput with both algorithms (WCICI & WOCICI) for 5 and 10 SRS periodicities and different UE speeds but for 20 ms SRS periodicity and medium and high UE speeds bot 1 SRSAS and 1SRSWOAS performs almost similarly.
- There is degradation of maximum cell throughput with increasing SRS periodicity and UE speed.

4.4.3. SU-MIMO vs. MU-MIMO (64 BS antenna elements and Full-Buffer traffic profile)

Table 4.10 summarizes Fig. 4.20, Fig. 4.38, and Fig. 4.40.

Table 4.10: Summary (Fig. 4.20, Fig. 4.38, and Fig. 4.40)

2SRS UE @ 64 BS antenna elements @5ms SRS periodicity @Full-Buffer		**Max_Thpt (bps) @3km/h @42users**	**Max_Thpt (bps) @30km/h @42users**
SU-MIMO	WOCICI	~52ε	~43ε
	WCICI	~80ε	~63ε
MU-MIMO @OF=0.1	WOCICI	~65ε	~48ε
	WCICI	~95ε	~68ε
MU-MIMO @OF=0.25	WOCICI	~82ε	~54ε
	WCICI	~125ε	~76ε
MU-MIMO @OF=1	WOCICI	~90ε	~56ε
	WCICI	~135ε	~80ε

From Table 4.10, the following observations can be made:

- In MU-MIMO with 64 BS antenna elements, both algorithms offer higher performance in terms of maximum cell throughput compared with the same algorithms in SU-MIMO with 64 BS antenna elements.
- In MU-MIMO, a higher value of orthogonality factor implies higher cell throughput for both algorithms.
- In general, there is degradation of maximum cell throughput with increasing UE speed.

5. Conclusions

The two discussed (in Chapter 4) algorithms for both SU-MIMO and MU-MIMO are:

- Algorithm 1: based on precoding that does not consider ICI (WOCICI).
- Algorithm 2: based on precoding that does consider ICI (WCICI).

Based on the obtained results, the following conclusions can be drawn for both algorithms:

5.1. SU-MIMO (FTP)

- WCICI performs better than WOCICI for pedestrian users (3 Km/h), for different SRS periodicities (5, 10 and 20 ms) and SRS UL antenna configurations. However, and under the specific traffic profiles used in the simulations, for medium (30 km/h) and high (60 km/h) UE speeds, it is better to use WOCICI since it performs similarly or better than WCICI.
- The performance of 1 SRSWOAS outperforms 1 SRSAS for medium and high UE speeds.
- In general, there is degradation of maximum cell throughput with increasing SRS periodicity and UE speed.

5.2. SU-MIMO (Full-Buffer)

- WCICI performs better than WOCICI for pedestrian users (3 Km/h), medium (30 km/h) and high moving speed (60 km/h), for different SRS periodicities (5, 10 and 20 ms) and SRS UL antenna configurations.
- The performances of 1 SRSWOAS and 1 SRSAS for high UE speed are almost the same.
- In general, there is degradation of maximum cell throughput with increasing SRS periodicity and UE speed.

5.3. MU-MIMO (Full-Buffer)

- In our simulations, it always best to have an orthogonality factor of one which means that we pair as many users as possible (maximum number of UEs can be paired. This is because users are dropped somewhat sparsely in the simulation area. With higher user loads, other values of the orthogonality factor might work better.
- WCICI case performs better WOCICI for low and medium load in the system.
- Similar to the SU-MIMO case, the cell throughput is decreased when the UE's speed is increased from 3 to 30 Km/h.

6. Future work

As already mentioned, this thesis work has been focusing on the following main aspects:

- Downlink SU/MU-MIMO
- Transmission mode: TM-8 (2 layers' transmission)
- 2 layers at the UE's side
- Traffic profile: Full-Buffer
- SRS bandwidth: 96x1 PRBs (Full-bandwidth SRS configuration)
- Scheduler: Round Robin (RR)

More aspects regarding scheduler algorithms for MU-MIMO not yet investigated include:

- Uplink SU/MU-MIMO
- 8 layers' transmission, i.e. TM-9/10
- 1 layer at the UE' side.
- Sub-bands SRS configuration i.e. 24x4 PRBs
- Other scheduling strategies such as Proportional Fair (PF), Max C/I and so on.
- Research proposals available in Section 1.4 (Previous related work).

References

[1] G. Bauch and G. Dietl, "Multi-user MIMO for achieving IMT-Advanced requirements," *2008 International Conference on Telecommunications*, St. Petersburg, 2008, pp. 1-7.

[2] F. Boccardi et al., "Multiple-antenna techniques in LTE-advanced," in IEEE Communications Magazine, vol. 50, no. 3, pp. 114-121, March 2012.

[3] L. Liu, R. Chen, S. Geirhofer, K. Sayana, Z. Shi and Y. Zhou, "Downlink MIMO in LTE-advanced: SU-MIMO vs. MU-MIMO," in *IEEE Communications Magazine*, vol. 50, no. 2, pp. 140-147, February 2012.

[4] C. Lim, T. Yoo, B. Clerckx, B. Lee and B. Shim, "Recent trend of multiuser MIMO in LTE-advanced," in *IEEE Communications Magazine*, vol. 51, no. 3, pp. 127-135, March 2013.

[5] Z. Lin, B. Vucetic and J. Mao, "Ergodic Capacity of LTE Downlink Multiuser MIMO Systems," *2008 IEEE International Conference on Communications*, Beijing, 2008, pp. 3345-3349.

[6] K. C. Beh, C. Han, M. Nicolaou, S. Armour and A. Doufexi, "Power Efficient MIMO Techniques for 3GPP LTE and Beyond," 2009 IEEE 70th Vehicular Technology Conference Fall, Anchorage, AK, 2009, pp. 1-5.

[7] W. Ajib and D. Haccoun, "An overview of scheduling algorithms in MIMO-based fourth-generation wireless systems," in IEEE Network, vol. 19, no. 5, pp. 43-48, Sept.-Oct. 2005.

[8] Yueming Cai, Jiang Yu, Youyun Xu and Mulin Cai, "A comparison of packet scheduling algorithms for OFDMA systems," 2008 2nd International Conference on Signal Processing and Communication Systems, Gold Coast, 2008, pp. 1-5.

[9] A. Farajidana, W. Chen, A. Damnjanovic, T. Yoo, D. Malladi and C. Lott, "3GPP LTE Downlink System Performance," GLOBECOM 2009 - 2009 IEEE Global Telecommunications Conference, Honolulu, HI, 2009, pp. 1-6.

[10] R. Kwan, C. Leung and J. Zhang, "Proportional Fair Multiuser Scheduling in LTE," in IEEE Signal Processing Letters, vol. 16, no. 6, pp. 461-464, June 2009.

[11] H. A. M. Ramli, R. Basukala, K. Sandrasegaran and R. Patachaianand, "Performance of well-known packet scheduling algorithms in the downlink 3GPP LTE system," 2009 IEEE 9th Malaysia International Conference on Communications (MICC), Kuala Lumpur, 2009, pp. 815-820.

[12] L. Liu, Young-Han Nam and J. Zhang, "Proportional fair scheduling for multi-cell multi-user MIMO systems," 2010 44th Annual Conference on Information Sciences and Systems (CISS), Princeton, NJ, 2010, pp. 1-6.
[13] D. Samia and B. Ridha, "A New Scheduling Algorithm for Real-Time Communication in LTE Networks," 2015 IEEE 29th International Conference on Advanced Information Networking and Applications Workshops, Gwangiu, 2015, pp. 267-271.
[14] Qurat-ul-Ain, S. R. ul Hassnain, M. Shah and S. A. Mahmud, "An evaluation of scheduling algorithms in LTE based 4G networks," 2015 International Conference on Emerging Technologies (ICET), Peshawar, 2015, pp. 1-6.
[15] A. Marinčić and D. Šimunić, "Performance evaluation of different scheduling algorithms in LTE systems," 2016 39th International Convention on Information and Communication Technology, Electronics and Microelectronics (MIPRO), Opatija, 2016, pp. 595-600.
[16] C. Johnson, Long Term Evolution in Bullets, second ed., Create Space Independent Publishing Platform, July 2012.
[17] 3GPP36.211, "Evolved Universal Terrestrial Radio Access (E-UTRA); Physical channels and modulation" 3GPP, Sophia Antipolis, Technical Specification 36.211 v13.2.0, August 2016.
[18] 3GPP36.212, "Evolved Universal Terrestrial Radio Access (E-UTRA); Multiplexing and channel coding" 3GPP, Sophia Antipolis, Technical Specification 36.212 v13.0.0, January 2016.
[19] 3GPP36.213, "Evolved Universal Terrestrial Radio Access (E-UTRA); Physical layer procedures" 3GPP, Sophia Antipolis, Technical Specification 36.213 v13.0.0, May 2016.
[20] E. Dahlman et al., 3G Evolution: HSPA and LTE for Mobile Broadband, 2nd ed., Academic Press, 2008.
[21] E. Dahlman, S. Parkvall, and J. Sköld, *4G: LTE/LTE Advanced for Mobile Broadband*, 2nd ed., Academic Press, 2014.
[22] E. Dahlman, S. Parkvall, and J. Sköld, *4G, LTE-Advanced Pro and The Road to 5G*, Academic Press, 2016.
[23] 3GPP TR 36.873," Technical Specification Group Radio Access Network; Study on 3D channel model for LTE" 3GPP, Sophia Antipolis, Technical Report 36.873 v12.3.0, December 2016.
[24] 3GPP TR 36.897," Technical Specification Group Radio Access Network; Study on elevation beamforming / Full-Dimension (FD) Multiple Input Multiple Output (MIMO) for LTE" 3GPP, Sophia Antipolis, Technical Report 36.897 v13.0.0, June 2015.

[25] 3GPP TR 25.996," Technical Specification Group Radio Access Network; Spatial channel model for Multiple Input Multiple Output (MIMO) simulations (Release 9)", 3GPP, Sophia Antipolis, *Technical Report* 25.996 V9.0.0, December 2009.

[26] Paulraj, Arogyaswami, Rohit Nabar, and Dhabanjay Gore, Introduction to Space-Time Wireless Communications, Cambridge, UK: Cambridge University Press, 2003.

[27] F. Capozzi, G. Piro, L. A. Grieco, G. Boggia and P. Camarda, "Downlink Packet Scheduling in LTE Cellular Networks: Key Design Issues and a Survey," in IEEE Communications Surveys & Tutorials, vol. 15, no. 2, pp. 678-700, Second Quarter 2013.

[28] G. Ku and J. M. Walsh, "Resource Allocation and Link Adaptation in LTE and LTE Advanced: A Tutorial," in IEEE Communications Surveys & Tutorials, vol. 17, no. 3, pp. 1605-1633, third-quarter 2015.

[29] 3GPP TR 36.814," Technical Specification Group Radio Access Network; Further Advancements for E-UTRA Physical Layer Aspects (Release 9)", 3GPP, Sophia Antipolis, *Technical Report* 36.814 V0.4.1, February 2009.

Appendices

Appendix 2.A: Uplink-downlink configurations for TDD radio frame [17]

Uplink-Downlink configuration	Downlink-to-Uplink Switch-point periodicity (ms)	Subframe number									
		0	1	2	3	4	5	6	7	8	9
0	5	D	S	U	U	U	D	S	U	U	U
1	5	D	S	U	U	D	D	S	U	U	D
2	5	D	S	U	D	D	D	S	U	D	D
3	10	D	S	U	U	U	D	D	D	D	D
4	10	D	S	U	U	D	D	D	D	D	D
5	10	D	S	U	D	D	D	D	D	D	D
6	5	D	S	U	U	U	D	S	U	U	D

Appendix 2.B: Transmission mode 8 (TM-8) in LTE (Downlink)

i. Single antenna port transmission

Single antenna port transmission can be realized according to [17] as follows:

- Only a single layer (υ = 1) and one codeword (q = 0) are available for transmission on a single antenna port
- Codeword-to-layer-mapping is defined by [17]:

$x^{(0)}(i) = d^{(0)}(i)$ with $M_{symb}^{layer} = M_{symb}^{(0)}$

where$x(i) = \left[x^{(0)}(i) \dots x^{(\upsilon-1)}(i)\right]^T, i = 0,1, \dots, M_{symb}^{layer} - 1$ are layers onto which modulation symbols $d^{(q)}(0), \dots, d^{(q)}\left(M_{symb}^{(q)} - 1\right)$ for

codeword q are mapped, υ is the number of layers, M_{symb}^{layer} is the number of modulation symbols per layer and $M_{symb}^{(q)}$ is the number of modulation symbols per codeword q.

- Precoding for downlink transmission on a single antenna port is defined by [17]:

$y^{(p)}(i) = x^{(0)}(i)$ for $i = 0,1,\dots,M_{symb}^{ap} - 1, M_{symb}^{ap} = M_{symb}^{layer}$ where

the transmission of the physical channel takes place on the following single antenna ports p ∈ {0,4,5,7,8,11,13} and. M_{symb}^{ap} is the number of modulation symbols per antenna port, $x^{(0)}(i)$ is the precoder input and $y^{(p)}(i)$ is the precoder output for antenna port p.

ii. Transmit Diversity

Downlink transmit diversity must satisfy the following conditions [17]:

- Only one codeword (q = 0) is available
- The number of layers υ is the same as the number of antenna ports P used for transmission i.e p = 2 when υ = 2 or p = 4 when υ = 4
- Downlink transmit diversity supports two or four antenna ports which are {0,1} and {0,1,2,3} respectively.

Downlink transmit diversity for 2 antenna ports {0,1} can be implemented according to [17] as follows:

- Codeword-to-layer mapping for 2 antenna ports {0,1} is defined by [17]:

$\begin{cases} x^{(0)}(i) = d^{(0)}(2i) \\ x^{(1)}(i) = d^{(0)}(2i+1) \end{cases}$ with $M_{symb}^{layer} = {M_{symb}^{(0)}}/{2}$ where

$x(i) = \left[x^{(0)}(i) \dots x^{(\upsilon-1)}(i)\right]^T, i = 0,1,\dots,M_{symb}^{layer} - 1$ are layers onto which modulation symbols $d^{(q)}(0),\dots,d^{(q)}\left(M_{symb}^{(q)} - 1\right)$ for codeword q are mapped, υ is the number of layers, M_{symb}^{layer} is the number of modulation symbols per layer and $M_{symb}^{(q)}$ is the number of modulation symbols per codeword q.

- Precoding operation for 2 antenna ports {0,1} is defined by [17]:

$$\begin{bmatrix} y^{(0)}(2i) \\ y^{(1)}(2i) \\ y^{(0)}(2i+1) \\ y^{(1)}(2i+1) \end{bmatrix} = \frac{1}{\sqrt{2}} \begin{bmatrix} 1 & 0 & j & 0 \\ 0 & -1 & 0 & j \\ 0 & 1 & 0 & j \\ 1 & 0 & -j & 0 \end{bmatrix} \begin{bmatrix} Re\left(x^{(0)}(i)\right) \\ Re\left(x^{(1)}(i)\right) \\ Im\left(x^{(0)}(i)\right) \\ Im\left(x^{(1)}(i)\right) \end{bmatrix} \text{ for}$$

$$i = 0,1,\dots,M_{symb}^{layer} - 1 \; with \; M_{symb}^{ap} = 2M_{symb}^{layer}.$$

$y(i) = \left[y^{(0)}(i)\; y^{(1)}(i)\right]^T, i = 0,1,\dots,M_{symb}^{ap} - 1$ is the precoder output and M_{symb}^{ap} is the number of modulation symbols per antenna port.

iii. Dual layer Beamforming

2x2 Closed loop downlink spatial multiplexing with 2 codewords and 2 layers for 2 antenna ports {0,1} can be implemented according to [17] as follows:

- Codeword-to-layer mapping for 2 antenna ports is defined by [17]:

$x^{(0)}(i) = d^{(0)}(i)$ with $M_{symb}^{layer} = M_{symb}^{(0)}$ for 1 codeword and 1 layer

$\begin{cases} x^{(0)}(i) = d^{(0)}(i) \\ x^{(1)}(i) = d^{(1)}(i) \end{cases}$ with $M_{symb}^{layer} = M_{symb}^{(0)} = M_{symb}^{(1)}$

for 2 codewords and 2 layers where $x(i) = \left[x^{(0)}(i) \dots x^{(\upsilon-1)}(i)\right]^T, i = 0,1,\dots,M_{symb}^{layer} - 1$ are layers onto which modulation symbols $d^{(q)}(0),\dots,d^{(q)}\left(M_{symb}^{(q)} - 1\right)$ for codeword q are mapped, υ is the number of layers, M_{symb}^{layer} is the number of modulation symbols per layer and $M_{symb}^{(q)}$ is the number of modulation symbols per codeword q.

- Precoding without Cyclic Delay Diversity (CDD)

Without CDD, precoding for spatial multiplexing is defined by [17]:

$$\begin{bmatrix} y^{(0)}(i) \\ . \\ . \\ y^{(P-1)}(i) \end{bmatrix} = W(i) \begin{bmatrix} x^{(0)}(i) \\ . \\ . \\ x^{(\upsilon-1)}(i) \end{bmatrix}$$

$$\text{with } i = 0,1,\dots,M_{symb}^{ap} - 1, M_{symb}^{ap} = M_{symb}^{layer}.$$

M_{symb}^{layer} is the number of modulation symbols per layer and M_{symb}^{ap} is the number of modulation symbols per antenna port. W(i) is the precoder matrix of size P x υ and different precoder matrices W(i) can be found in the e-Node B and the UE where they are configured according to table 1. For dual layer beamforming, 2 layers are used i.e. υ = 2.

Table 2.B: Precoder matrices for two antenna ports (Downlink spatial multiplexing) [17]

Codebook index		0	1	2	3
Number of layers υ	1	$\frac{1}{\sqrt{2}}\begin{bmatrix}1\\1\end{bmatrix}$	$\frac{1}{\sqrt{2}}\begin{bmatrix}1\\-1\end{bmatrix}$	$\frac{1}{\sqrt{2}}\begin{bmatrix}1\\j\end{bmatrix}$	$\frac{1}{\sqrt{2}}\begin{bmatrix}1\\-j\end{bmatrix}$
	2	$\frac{1}{\sqrt{2}}\begin{bmatrix}1 & 0\\0 & 1\end{bmatrix}$	$\frac{1}{2}\begin{bmatrix}1 & 1\\1 & -1\end{bmatrix}$	$\frac{1}{2}\begin{bmatrix}1 & 1\\j & -j\end{bmatrix}$	-

The following steps are need for dual layer beamforming [16]:

- Codewords/UE specific reference signals to resource grid mapping (codeword 1 and UE specific reference signal for antenna port 7 per resource grid and codeword 2 and UE specific reference signal for antenna port 8 per resource grid
- Complex weights calculation from uplink SRS using channel estimation
- Antenna ports to antenna element mapping: Antenna port 7 is mapped to $+45^0$ polarization antenna elements while antenna port 8 is mapped to -45^0 polarization antenna elements

Printed by Tryckeriet i E-huset, Lund 2017

LUND
UNIVERSITY

Series of Master's theses
Department of Electrical and Information Technology
LU/LTH-EIT 2017-606

http://www.eit.lth.se